UNIVERSITY
OF
QUEENSLAND

Department of Civil Engineering

RESEARCH REPORT SERIES

Large Deflection and Post-Buckling Analysis of Two and Three Dimensional Elastic Spatial Frames

J. L. MEEK and

H. S. TAN

FRY,
TA
1
.U4956
NO.49
1

esearch Report No. CE49
December, 1983

TA
1
.U4956
no. 49
1
FRYER

3 4067 03257 5614

CIVIL ENGINEERING RESEARCH REPORTS

This report is one of a continuing series of Research Reports published by the Department of Civil Engineering at the University of Queensland. This Department also publishes a continuing series of Bulletins. Lists of recently published titles in both of these series are provided inside the back cover of this report. Requests for copies of any of these documents should be addressed to the Departmental Secretary.

The interpretations and opinions expressed herein are solely those of the author(s). Considerable care has been taken to ensure the accuracy of the material presented. Nevertheless, responsibility for the use of this material rests with the user.

Department of Civil Engineering,
University of Queensland,
St Lucia, Q 4067, Australia,
[Tel:(07) 377-3342, Telex:UNIVQLD AA40315]

LARGE DEFLECTION AND POST-BUCKLING ANALYSIS OF TWO AND THREE DIMENSIONAL ELASTIC SPATIAL FRAMES

by

J.L. MEEK, MS *Calif.*, BE, BSc, PhD,
Associate Professor of Civil Engineering

and

H. S. TAN, BSc, ACGI,
Post Graduate Student

RESEARCH REPORT NO. CE 49
Department of Civil Engineering
University of Queensland
December, 1983

Synopsis

The safe and economical design of curved spatial frames necessitates a geometrical nonlinear analysis of the structure. In this report, the nonlinear equations governing such structural behaviour are derived. Solution strategies which are capable of analysing the post-buckling behaviour of structures are also critically reviewed. In addition, an extrapolation stiffness method that lends itself to a more efficient solution of the nonlinear equations than conventional Newton-Raphson methods is presented.

The post-buckling responses of various spatial frames are analysed and the results found to be in good agreement with available published work.

UNIVERSITY OF QUEENSLAND LIBRARY

CONTENTS

Reg. exchange
1984
Fryer

		Page
1.	INTRODUCTION	1
2.	DERIVATION OF GOVERNING NONLINEAR EQUATIONS	3
	2.1 GOVERNING EQUATIONS FOR PLANE FRAME	7
	2.1.1 Member basic force-displacement relation	7
	2.2 GOVERNING EQUATIONS FOR SPACE FRAMES	12
	2.2.1 Member basic force-displacement relation	12
	2.2.2 Transformation from Member Basic Force/ Displacements to Member Nodal Force/ Displacement (Local Co-ordinates)	16
	2.2.3 Transformation from Member Co-ordinates to Global Co-ordinates	22
	2.2.4 Evaluation of Member Rotational Deformations from Joint Orientation Matrix	23
3.	SOLUTION STRATEGIES FOR TRAVERSING LIMIT POINTS	25
4.	CONSTANT ARC LENGTH STRATEGY OF CRISFIELD	33
5.	EVALUATION OF POST-BIFURCATION EQUILIBRIUM PATH (SECONDARY PATH)	36
6.	EXTRAPOLATED STIFFNESS PROCEDURE	40
7.	NUMERICAL EXAMPLES	42
	7.1 CANTILEVER BEAM	42
	7.2 WILLIAMS' TOGGLE FRAME	42
	7.3 TWELVE MEMBER HEXAGONAL SPACE FRAME	45
	7.4 TWENTY-FOUR MEMBER STAR-SHAPED DOME	50
8.	CONCLUSION	50
APPENDIX A	- NOMENCLATURE	52
APPENDIX B	- REFERENCES	56

1. INTRODUCTION

Curved structural space frames belong to a class of structures where a large proportion of the applied loading is resisted by the axial forces in the members. This together with the trend towards optimum light weight members, for reasons of economy and aesthetics, has brought to the fore the stability analysis of this type of structure, as it is inclined to fail through elastic instability before exhibiting any significant nonlinear material response. The elastic buckling load has in the main been calculated using linear instability theory, through a linearised eigenvalue approach. For structures where the pre-buckling path is linear or close to being linear, this method will suffice. However, in the presence of initial imperfections and geometric nonlinearities, this procedure can grossly overestimate the actual buckling load. In addition, the information furnished by a linearised eigenvalue analysis is limited. The pre-buckling load-deflection path is not traced out and more importantly the nature of the bifurcation failure, whether the failure is catastrophic or there is an increase in post buckling stiffness as the structure deforms further, is not known. These considerations lead us to the desirability of considering the geometrical nonlinearities when formulating the equilibrium equations, the result of which is a system of nonlinear equations.

The formulation of the nonlinear equations governing the large deflection behaviour of framed structures has been extensively studied by various authors and is based on either the finite element method [1-5] or on the 'beam-column' approach [6-13]. In describing the motion of the element, a total Lagrangian or an updated Lagrangian description can be employed. The finite element formulation is generally used in conjunction with a total Lagrangian material description. Analyses based

on this approach are however limited by the magnitude of the joint rotations. To overcome this problem of large joint rotations, an updated Lagrangian approach can be employed which separates the effects of pure member deformations from the joint displacements. This is achieved by introducing a local, convective reference system attached to the member.

The nonlinear equations can be solved by utilising the unconstrained minimisation algorithms of mathematical programming. All the geometrical nonlinearities are included in the potential energy functional which is then minimised. Techniques such as the random search method [14] and Powell's method of conjugate direction [15] utilise the object function only; the method of steepest descent [14] and the conjugate gradient method [16], in addition makes use of the gradient (first derivative); while the quasi-Newton [17-19], secant-Newton [20] and Newton-Raphson [21] require the evaluation of the 2nd derivates as well. This approach has been adopted by Berke and Mallet [2] as early as 1969, and more recently by Papadrakakis [13] and Kamat [22] to trace the complete load-deflection path of spatial framed structures.

An alternative to solving the nonlinear equations lies in using an incremental form of the equilibrium equations. The linearised incremental-iterative techniques appear to be more efficient than the minimisation methods for large scale problems. It however, breaks down at the first onset of instability due to the singularity of the incremental stiffness matrix. Earlier work on the large deflection behaviour of framed structures employing an incremental iterative method has thus been limited to studying their prebuckling behaviour [8-10,23] and it is only very recently that robust and efficient techniques that circumvent this problem have been developed. Several good reviews of these

techniques for traversing the limit points exist in the literature [24-27]. These solution strategies have invariably been applied to the analysis of thin shell structures. To the authors' knowledge the only published work utilising these nonlinear solution strategies to spatial frames is that of Reference [4,28] on two-dimensional frames and of Reference [5] on three-dimensional frames; where only limited examples were presented. There is thus scope for further work in applying these newly developed nonlinear solution strategies to analysing the post-buckling response of spatial frames.

In the linearised incremental-iterative technique, equilibrium iterations are performed within each increment. In the Newton-Raphson (NR) method, each iteration would entail the assembly and factorisation of the tangent stiffness matrix. This is, however, very expensive and in practise the tangent stiffness is kept constant throughout the increment or is changed only after a few iterative cycles. More iterations will be needed for the modified Newton-Raphson method (mNR), but this may more than outweigh the cost of reforming and refactorising the incremental stiffness matrix at every cycle. The authors in Reference [29] have developed an extrapolated stiffness strategy which was found to be more efficient than the mNR or NR methods, when tested for plane frames. The applicability of the conclusions reached in Reference [29], to three-dimensional frames is also demonstrated in this report.

2. DERIVATION OF GOVERNING NONLINEAR EQUATIONS

The 'beam-column' approach has been used here in deriving the governing nonlinear equations. Here in the members are assumed to be of constant cross-section with the external loads applied only at the joints. Only conservative or displacement independent loading is considered.

Shear deformations are neglected and the material is assumed to be linearly elastic. For the three-dimensional frames, the members' cross-sections are doubly symmetric, thus excluding coupling of the torsional stiffness to that of the bending and axial stiffness. Warping effects are also neglected.

In developing the nonlinear equations, two types of co-ordinate systems are employed; a fixed global set of co-ordinates and a local convective system which rotates and translates with the member. The member deformations are thus separated from the joint displacements. The basic member force-deformation relations are derived in the local convective co-ordinates with member deformations assumed to be small relative to it, through the principle of minimum potential energy. This formulation of the equilibrium equation through an updated Lagrangian approach is thus applicable to analysing structures exhibiting large rotation small strain behaviour. The member forces and displacements in the various co-ordinate systems are illustrated in Figures 1 and 2 for the two and three-dimensional frames respectively.

The rotational degrees of freedom are described by Euler angles for the case of the two-dimensional frames. Due to the occurence of large rotations in post-buckling analysis, this description by Euler angles is unsatisfactory for the analysis of three-dimensional space frames. This stems from the fact that finite rotations in three-dimensional space are non-vectorial quantities in that they do no comply with the rules of vector transformation. To overcome this difficulty, the concept of a joint orientation matrix comprising of a triad of orthogonal unit vectors as presented in References [12 and 30] is employed to describe the arbitrary large nodal rotations.

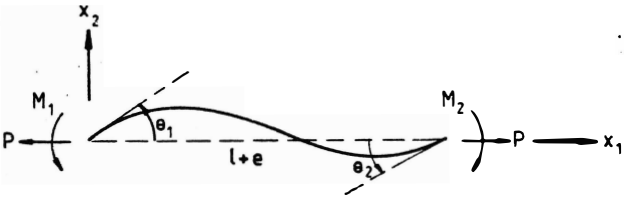

(a) Member basic displacements and forces

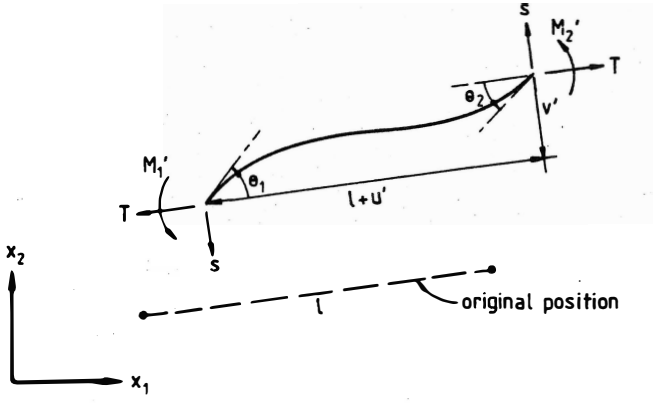

(b) Member intermediate displacements and forces

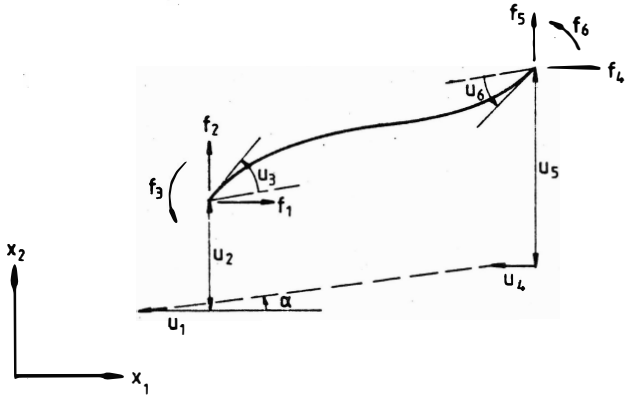

(c) Member nodal forces and displacements
(global co-ordinates)

Figure 1. Member deformations and associated forces
(2-dimensional frame)

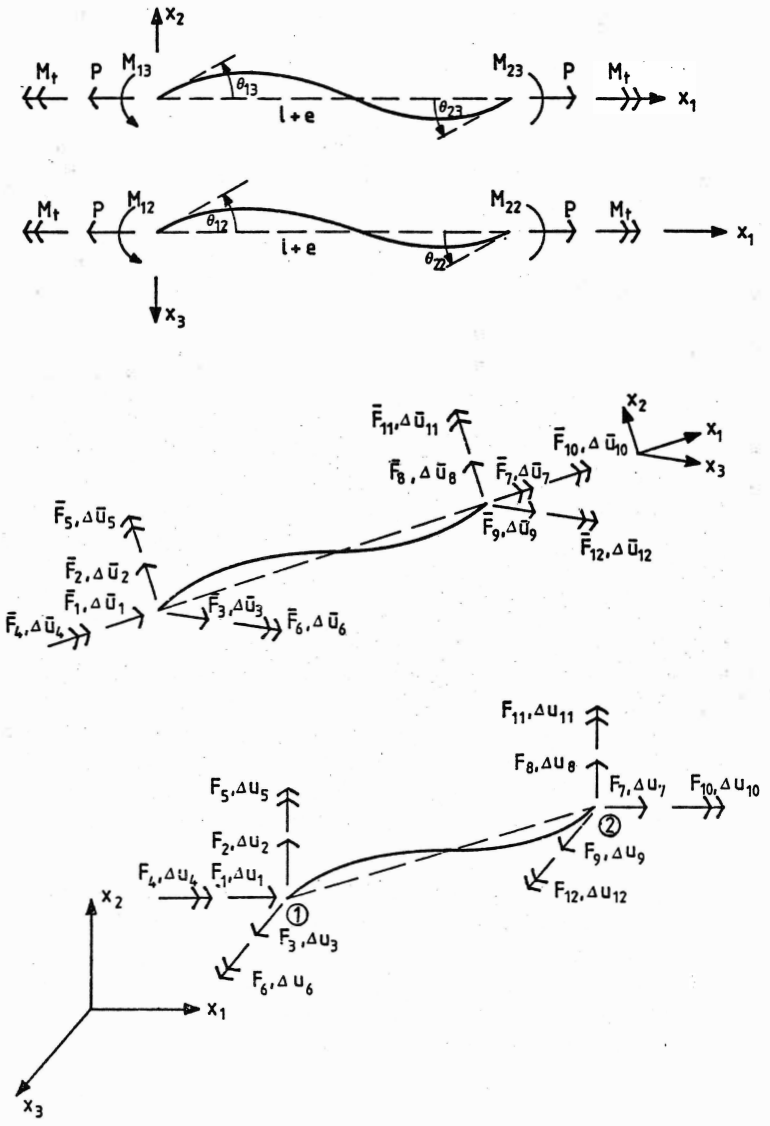

Figure 2. Member deformations and associated forces (3-dimensional frame)

2.1 GOVERNING EQUATIONS FOR PLANE FRAMES

2.1.1 Member basic force-displacement relation

On assuming a cubic lateral deflection curve and that the axial deformation, e is small compared to the original member length, ℓ

$$x_2 = \theta_1\left(x_1 - \frac{2x_1^2}{\ell} + \frac{x_1^3}{\ell^2}\right) + \theta_2\left(-\frac{x_1^2}{\ell} + \frac{x_1^3}{\ell^2}\right) \tag{1}$$

and the axial lengthening due to bowing is

$$u_b = \frac{1}{2}\int_0^{\ell}\left(\frac{dx_2}{dx_1}\right)^2 dx_1 \tag{2}$$

$$= \frac{\ell}{30}\left(2\theta_1^2 - \theta_1\theta_2 + 2\theta_2^2\right)$$

The axial load, P is thus

$$P = EA\left[\frac{e}{\ell} + \frac{1}{30}\left(2\theta_1^2 - \theta_1\theta_2 + 2\theta_2^2\right)\right] \tag{3}$$

where EA = axial rigidity. Neglecting the shear strain energy, the potential energy due to lateral deflection along the prinicipal axis is

$$\Psi = \frac{1}{2}\int_0^{\ell} EI\left(\frac{d^2x_2}{dx_1^2}\right)^2 dx_1 - M_1\theta_1 - M_2\theta_2 + P\left(\frac{1}{2}\int_0^{\ell}\left(\frac{dx_2}{dx_1}\right)^2 dx_1\right) \tag{4}$$

Through the principle of minimum potential energy, the member forces are thus,

$$M_1 = \left(\frac{4EI}{\ell} + \frac{4P\ell}{30}\right)\theta_1 + \left(\frac{2EI}{\ell} - \frac{P\ell}{30}\right)\theta_2 \tag{5}$$

$$M_2 = \left(\frac{2EI}{\ell} - \frac{P\ell}{30}\right)\theta_1 + \left(\frac{4EI}{\ell} + \frac{4P\ell}{30}\right)\theta_2$$

where EI = flexural rigidity

The basic incremental stiffness matrix is obtained by partial differentiating Equations (3) and (5) with respect to the member basic deformations. Hence

$$\begin{bmatrix} dP \\ dM_1 \\ dM_2 \end{bmatrix} = \begin{bmatrix} \frac{EA}{\ell} & \frac{EA}{30}\left(4\theta_1 - \theta_2\right) & \frac{EA}{30}\left(-\theta_1 + 4\theta_2\right) \\ & k_{22} & k_{23} \\ \text{symmetric} & & k_{33} \end{bmatrix} \begin{bmatrix} de \\ d\theta_1 \\ d\theta_2 \end{bmatrix}$$

where

$$k_{22} = \frac{4EI}{\ell} + \frac{4EAe}{30} + \frac{EA\ell}{300}\left(8\theta_1^2 - 4\theta_1\theta_2 + 3\theta_2^2\right)$$

$$k_{23} = \frac{2EI}{\ell} - \frac{EAe}{30} + \frac{EA\ell}{300}\left(-2\theta_1^2 + 6\theta_1\theta_2 - 2\theta_2^2\right)$$

$$k_{33} = \frac{4EI}{\ell} + \frac{4EAe}{30} + \frac{EA\ell}{300}\left(3\theta_1^2 - 4\theta_1\theta_2 + 8\theta_2^2\right)$$

$$\therefore \quad \{\Delta \underset{\sim}{s}\} = [\underset{\sim}{k}]\{\Delta \underset{\sim}{v}\} \qquad (6)$$

2.1.2 Transformation from member basic force displacement to member intermediate force/displacement

Considering gross deformation,

$$e = \sqrt{(\ell + u')^2 + v'^2} - \ell$$

$$\theta_1 = \theta'_1 - \tan^{-1}\left(\frac{v'}{\ell + u'}\right)$$

$$\theta_2 = \theta'_2 - \tan^{-1}\left(\frac{v'}{\ell + u'}\right) \qquad (7)$$

On partial differentiating,

$$de = \left\{\frac{1}{2}\left[(\ell + u')^2 + v'^2\right]^{-\frac{1}{2}} 2(\ell + u')\right\} du'$$

$$+ \left\{\frac{1}{2}\left[(\ell + u')^2 + v'^2\right]^{-\frac{1}{2}} 2v'\right\} dv' + (0)\, d\theta'_1 + (0)\, d\theta'_2$$

$$d\theta_1 = \frac{v'}{(\ell + e)^2}\, du' - \frac{\ell + u'}{(\ell + e)^2}\, dv' + (1)\, d\theta'_1 + (0)\, d\theta'_2$$

$$d\theta_2 = \frac{v'}{(\ell + e)^2}\, du' - \frac{\ell + u'}{(\ell + e)^2}\, dv' + (0)\, d\theta'_1 + (1)\, d\theta'_2$$

Thus

$$\begin{bmatrix} de \\ d\theta_1 \\ d\theta_2 \end{bmatrix} = \begin{bmatrix} \frac{\ell + u'}{\ell + e} & \frac{v'}{\ell + e} & 0 & 0 \\ \frac{v'}{(\ell + e)^2} & -\frac{\ell + u'}{(\ell + e)^2} & 1 & 0 \\ \frac{v'}{(\ell + e)^2} & -\frac{\ell + u'}{(\ell + e)^2} & 0 & 1 \end{bmatrix} \begin{bmatrix} du' \\ dv' \\ d\theta' \\ d\theta'_2 \end{bmatrix}$$

$$\therefore \quad \{\Delta \underset{\sim}{v}\} = [\underset{\sim}{A}]\ \{\Delta \underset{\sim}{u}'\} \tag{8}$$

By the contragredient principle

$$\{\underset{\sim}{f}'\} = [\underset{\sim}{A}]^T\ \{\underset{\sim}{s}\} \tag{9}$$

where

$$\{\underset{\sim}{f}'\}^T = \{T,\ S,\ M'_1,\ M'_2\}$$

and

$$\{\underset{\sim}{s}\}^T = \{P, M_1, M_2\}$$

On differentiating Equation (9)

$$\{\Delta\underset{\sim}{f}'\} = [A]^T \{\Delta\underset{\sim}{s}\} + [\underset{\sim}{D}] \{\Delta\underset{\sim}{u}'\} \tag{10}$$

where

$$[\underset{\sim}{D}] = \begin{bmatrix} d_{11} & d_{12} & 0 & 0 \\ d_{21} & d_{22} & 0 & 0 \\ 0 & 0 & 0 & 0 \\ 0 & 0 & 0 & 0 \end{bmatrix}$$

and

$$d_{11} = \frac{1}{(\ell + e)^4} \left[-v'^2(\ell + u') T + \left(2(\ell + u')^2 + v'^2\right) v'S \right]$$

$$d_{12} = d_{21} = \frac{1}{(\ell + e)^4} \left[-v'^3 T - (\ell + u')^3 S \right]$$

$$d_{22} = \frac{1}{(\ell + e)^4} \left[(\ell + u') \left((\ell + u')^2 + 2v'^2\right) T - (\ell + u')^2 v'S \right]$$

2.1.3 Transformation from member intermediate force/displacement to nodal global force/displacement

The member intermediate displacements are related to the nodal displacements by

$$\begin{bmatrix} u' \\ v' \\ \theta'_1 \\ \theta'_2 \end{bmatrix} = \begin{bmatrix} -\cos\alpha & -\sin\alpha & 0 & \cos\alpha & \sin\alpha & 0 \\ \sin\alpha & -\cos\alpha & 0 & -\sin\alpha & \cos\alpha & 0 \\ 0 & 0 & 1 & 0 & 0 & 0 \\ 0 & 0 & 0 & 0 & 0 & 1 \end{bmatrix} \begin{bmatrix} u_1 \\ u_2 \\ u_3 \\ u_4 \\ u_5 \\ u_6 \end{bmatrix}$$

$$\therefore \{\underset{\sim}{u}'\} = [\underset{\sim}{T}]\ \{\underset{\sim}{u}\} \tag{11}$$

and

$$\{\Delta\underset{\sim}{u}'\} = [\underset{\sim}{T}]\ \{\Delta\underset{\sim}{u}\} \tag{12}$$

By the contragredient principle,

$$\{\Delta\underset{\sim}{f}\} = [\underset{\sim}{T}]^T ([\underset{\sim}{A}]^T \{\Delta\underset{\sim}{s}\} + [\underset{\sim}{D}]\ \{\Delta\underset{\sim}{u}'\})$$

$$= [\underset{\sim}{T}]^T ([\underset{\sim}{A}]^T [\underset{\sim}{k}]\ \{\Delta\underset{\sim}{v}\} + [\underset{\sim}{D}]\ \{\Delta\underset{\sim}{u}'\})$$

$$= [\underset{\sim}{T}]^T ([\underset{\sim}{A}]^T [\underset{\sim}{k}]\ [\underset{\sim}{A}]\ \{\Delta\underset{\sim}{u}'\} + [\underset{\sim}{D}]\ \{\Delta\underset{\sim}{u}'\})$$

$$= [\underset{\sim}{T}]^T ([\underset{\sim}{A}]^T [\underset{\sim}{k}]\ [\underset{\sim}{A}] + [\underset{\sim}{D}])\ [\underset{\sim}{T}]\ \{\Delta\underset{\sim}{u}\}$$

$$= [\underset{\sim}{k}_G]\ \{\Delta\underset{\sim}{u}\} \tag{15}$$

2.2 GOVERNING EQUATIONS FOR SPACE FRAMES

2.2.1 Member basic force-displacement relation

In deriving the member basic force-deformation relation, it is assumed that the lateral deflection curve is cubic in each of the two principal directions, and that e is small relative to ℓ. Therefore

$$x_2 = \theta_{13}\left(x_1 - \frac{2x_1^2}{\ell} + \frac{x_1^3}{\ell^2}\right) + \theta_{23}\left(-\frac{x_1^2}{\ell} + \frac{x_1^3}{\ell^2}\right)$$

and

$$x_3 = \theta_{12}\left(x_1 - \frac{2x_1^2}{\ell} + \frac{x_1^3}{\ell^2}\right) + \theta_{22}\left(-\frac{x_1^2}{\ell} + \frac{x_1^3}{\ell^2}\right) \tag{16}$$

with the axial lengthening due to bowing being

$$u_b = \frac{1}{2}\int_0^{\ell}\left(\frac{dx_2}{dx_1}\right)^2 dx_1 + \frac{1}{2}\int_0^{\ell}\left(\frac{dx_3}{dx_1}\right)^2 dx_1$$

$$= \frac{\ell}{30}\left(2\theta_{13}^2 - \theta_{13}\theta_{23} + 2\theta_{23}^2\right) + \frac{\ell}{30}\left(2\theta_{12}^2 - \theta_{12}\theta_{22} + 2\theta_{22}^2\right) \tag{17}$$

The potential energy functional due to lateral deflection along the two principle axis, neglecting the shear strain, is

$$\Psi = \frac{1}{2}\int^{\ell} EI_3\left(\frac{d^2x_2}{dx_1^2}\right)^2 dx_1 + \frac{1}{2}\int_0^{\ell} EI_2\left(\frac{d^2x_3}{dx_1^2}\right)^2 dx_1 - M_{13}\theta_{13} - M_{23}\theta_{23} - M_{12}\theta_{12}$$

$$- M_{22}\theta_{22} + P\left[\frac{1}{2}\int_0^{\ell}\left(\frac{dx_2}{dx_1}\right)^2 dx_1 + \frac{1}{2}\int_0^{\ell}\left(\frac{dx_3}{dx_1}\right)^2 dx_1\right]$$

$$= \frac{2EI_3}{\ell^3}\theta_{13}^2 + \frac{2EI_3}{\ell^3}\theta_{13}\theta_{23} + \frac{2EI_3}{\ell^3}\theta_{23}^2 + \frac{2EI_2}{\ell^2}\theta_{12}^2 + \frac{2EI_2}{\ell^2}\theta_{12}\theta_{22}$$

$$+ \frac{2EI_2}{\ell^2}\theta_{22}^2 - M_{13}\theta_{13} - M_{23}\theta_{23} - M_{12}\theta_{12} - M_{22}\theta_{22}$$

$$+ \frac{P\ell}{30}\left[(2\theta_{12}^2 - \theta_{12}\theta_{23} + 2\theta_{23}^2) + (2\theta_{12}^2 - \theta_{12}\theta_{23} + 2\theta_{22}^2)\right] \qquad (18)$$

Through the principle of minimum potential energy, this leads us to

$$M_{13} = \left(\frac{4EI_3}{\ell} + \frac{4P\ell}{30}\right)\theta_{13} + \left(\frac{2EI_3}{\ell} - \frac{P\ell}{30}\right)\theta_{23}$$

$$M_{23} = \left(\frac{2EI_3}{\ell} - \frac{P\ell}{30}\right)\theta_{13} + \left(\frac{4EI_3}{\ell} + \frac{4P\ell}{30}\right)\theta_{23}$$

$$M_{12} = \left(\frac{4EI_2}{\ell} + \frac{4P\ell}{30}\right)\theta_{12} + \left(\frac{2EI_2}{\ell} - \frac{P\ell}{30}\right)\theta_{22}$$

$$M_{22} = \left(\frac{2EI_2}{\ell} - \frac{P\ell}{30}\right)\theta_{12} + \left(\frac{4EI_2}{\ell} + \frac{4P\ell}{30}\right)\theta_{22} \qquad (19)$$

where EI_2 and EI_3 are the flexural rigidities about the x_2 and x_3 axis respectively. The torsional moment and the axial force is given by

$$M_t = \frac{GJ}{\ell}\theta_t$$

$$P = EA\,\frac{e}{\ell} + \frac{1}{30}(2\theta_{13}^2 - \theta_{13}\theta_{23} + 2\theta_{23}^2) + \frac{1}{30}(2\theta_{12}^2 - \theta_{12}\theta_{22} + 2\theta_{22}^2) \qquad (20)$$

where EA = axial rigidity and GJ = torsional rigidity.

Partial differentiating Equations (19) and (20) with respect to the basic member deformations will lead us to the incremental stiffness matrix in the convected co-ordinate system.

Thus

$$\begin{bmatrix} \Delta M_{13} \\ \Delta M_{23} \\ \Delta M_{12} \\ \Delta M_{22} \\ \Delta M_t \\ \Delta P \end{bmatrix} = \begin{bmatrix} K_{11} & K_{12} & K_{13} & K_{14} & K_{15} & K_{16} \\ & K_{22} & K_{23} & K_{24} & K_{25} & K_{26} \\ & & K_{33} & K_{34} & K_{35} & K_{36} \\ & & & K_{44} & K_{45} & K_{46} \\ & \text{Symmetry} & & & K_{55} & K_{56} \\ & & & & & K_{66} \end{bmatrix} \begin{bmatrix} \Delta\theta_{13} \\ \Delta\theta_{23} \\ \Delta\theta_{12} \\ \Delta\theta_{22} \\ \Delta\theta_t \\ \Delta e \end{bmatrix}$$

where

$$K_{11} = \frac{4EI}{\ell^3} + \frac{4EAe}{30} + \frac{EA\ell}{300}(8\theta_{13}^2 - 4\theta_{13}\theta_{23} + 3\theta_{23}^2) + \frac{EA\ell}{900}(8\theta_{12}^2 - 4\theta_{12}\theta_{22} + 8\theta_{22}^2)$$

$$K_{12} = \frac{2EI}{\ell^3} - \frac{EAe}{30} - \frac{EA\ell}{300}(2\theta_{13}^2 - 6\theta_{13}\theta_{23} + 2\theta_{23}^2) - \frac{EA\ell}{900}(2\theta_{12}^2 - \theta_{12}\theta_{22} + 2\theta_{22}^2)$$

$$K_{13} = \frac{EA\ell}{900}(16\theta_{13}\theta_{12} - 4\theta_{13}\theta_{22} - 4\theta_{12}\theta_{23} + \theta_{23}\theta_{22})$$

$$K_{14} = \frac{EA\ell}{900}(-4\theta_{13}\theta_{12} + 16\theta_{13}\theta_{22} + \theta_{23}\theta_{12} - 4\theta_{23}\theta_{22})$$

$$K_{15} = 0.0$$

$$K_{16} = \frac{EA}{30}(4\theta_{13} - \theta_{23})$$

$$K_{22} = \frac{4EI}{\ell^3} + \frac{4EAe}{30} + \frac{EA\ell}{300}(3\theta_{13}^2 - 4\theta_{13}\theta_{23} + 8\theta_{23}^2)$$

$$+ \frac{EA\ell}{900}(8\theta_{12}^2 - 4\theta_{12}\theta_{22} + 8\theta_{22}^2)$$

$$K_{23} = \frac{EA\ell}{900}(-4\theta_{12}\theta_{13} + \theta_{13}\theta_{22} + 16\theta_{23}\theta_{12} - 4\theta_{23}\theta_{22})$$

$$K_{24} = \frac{EA\ell}{900}(\theta_{13}\theta_{12} - 4\theta_{13}\theta_{22} - 4\theta_{23}\theta_{12} + 16\theta_{23}\theta_{22})$$

$$K_{25} = 0.0$$

$$K_{26} = \frac{EA}{30}(-\theta_{13} + 4\theta_{23})$$

$$K_{33} = \frac{4EI}{\ell^2} + \frac{4EAe}{30} + \frac{EA\ell}{900}(8\theta_{13}^2 - 4\theta_{12}\theta_{23} + 8\theta_{23}^2)$$

$$+ \frac{EA\ell}{300}(8\theta_{12}^2 - 4\theta_{12}\theta_{22} + 3\theta_{22}^2)$$

$$K_{34} = \frac{2EI}{\ell^2} - \frac{EAe}{30} - \frac{EA\ell}{900}(2\theta_{13}^2 - \theta_{13}\theta_{23} + 2\theta_{23}^2)$$

$$- \frac{EA\ell}{300}(2\theta_{12}^2 - 6\theta_{12}\theta_{22} + 2\theta_{22}^2)$$

$$K_{35} = 0.0$$

$$K_{36} = \frac{EA}{30}(4\theta_{12} - \theta_{22})$$

$$K_{44} = \frac{4EI}{\ell^2} + \frac{4EAe}{30} + \frac{EA\ell}{900}(8\theta_{13}^2 - 4\theta_{13}\theta_{23} + 8\theta_{23}^2)$$

$$+ \frac{EA\ell}{300}(3\theta_{12}^2 - 4\theta_{12}\theta_{22} + 8\theta_{22}^2)$$

$$K_{45} = 0.0$$

$$K_{46} = \frac{EA}{30}(-\theta_{12} + 4\theta_{22})$$

$$K_{55} = \frac{GJ}{\ell}$$

$$K_{56} = 0.0$$

$$K_{66} = \frac{EA}{\ell}$$

$$\therefore \quad \{\Delta S\} = [K]\{\Delta V\} \tag{21}$$

2.2.2 Transformation from Member Basic Force/Displacements to Member Nodal Force/Displacement (Local Co-ordinates)

From considerations of geometry and equilibrium,

$$\begin{bmatrix} \bar{F}_1 \\ \bar{F}_2 \\ \bar{F}_3 \\ \bar{F}_4 \\ \bar{F}_5 \\ \bar{F}_6 \\ \bar{F}_7 \\ \bar{F}_8 \\ \bar{F}_9 \\ \bar{F}_{10} \\ \bar{F}_{11} \\ \bar{F}_{12} \end{bmatrix} = \begin{bmatrix} 0 & 0 & 0 & 0 & 0 & -1 \\ \frac{1}{\ell} & \frac{1}{\ell} & 0 & 0 & 0 & 0 \\ 0 & 0 & -\frac{1}{\ell} & -\frac{1}{\ell} & 0 & 0 \\ 0 & 0 & 0 & 0 & -1 & 0 \\ 0 & 0 & 1 & 0 & 0 & 0 \\ 1 & 0 & 0 & 0 & 0 & 0 \\ 0 & 0 & 0 & 0 & 0 & 1 \\ -\frac{1}{\ell} & -\frac{1}{\ell} & 0 & 0 & 0 & 0 \\ 0 & 0 & \frac{1}{\ell} & \frac{1}{\ell} & 0 & 0 \\ 0 & 0 & 0 & 0 & 1 & 0 \\ 0 & 0 & 0 & 1 & 0 & 0 \\ 0 & 1 & 0 & 0 & 0 & 0 \end{bmatrix} \begin{bmatrix} M_{13} \\ M_{23} \\ M_{12} \\ M_{22} \\ M_t \\ P \end{bmatrix}$$

$$\{\bar{F}\} = [B]\{S\} \tag{22}$$

Using the contragredient principle,

$$\{\Delta V\} = [B]^T \{\Delta\bar{u}\} \tag{23}$$

By differentiating Equation (22), its incremental form is obtained,

$$\{\Delta\bar{F}\} = [B]\{\Delta S\} + [\Delta B]\{S\} \tag{24}$$

The matrix $[\Delta B]$ is the change in $[B]$ resulting from $\{\Delta\bar{u}\}$. To evaluate $[\Delta B]$ let us consider the member moving from position (I) to (II) in Figure 3, which is equivalent to rotating the translational forces by

$$\rho_1 = 0; \qquad \rho_2 = -\frac{(\Delta\bar{u}_9 - \Delta\bar{u}_3)}{\ell}; \qquad \rho_3 = \frac{(\Delta\bar{u}_8 - \Delta\bar{u}_2)}{\ell} \tag{25}$$

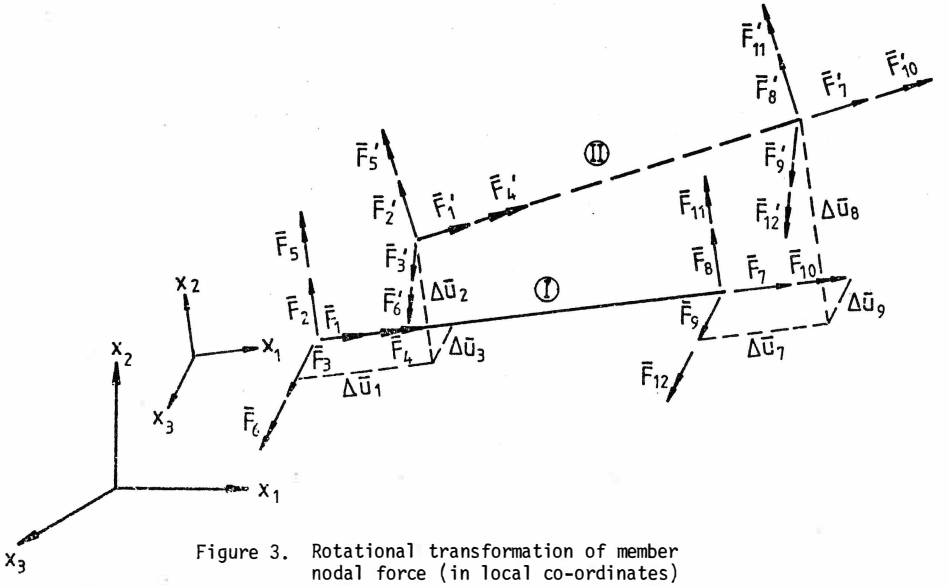

Figure 3. Rotational transformation of member nodal force (in local co-ordinates)

about the member axis. The nodal forces in local co-ordinates are thus

$$\begin{bmatrix} F'_1 \\ F'_2 \\ F'_3 \\ F'_4 \\ F'_5 \\ F'_6 \\ F'_7 \\ F'_8 \\ F'_9 \\ F'_{10} \\ F'_{11} \\ F'_{12} \end{bmatrix} \quad \begin{bmatrix} 1 & -\rho_3 & \rho_2 & 0 & 0 & 0 & 0 & 0 & 0 & 0 & 0 & 0 \\ \rho_3 & 1 & 0 & 0 & 0 & 0 & 0 & 0 & 0 & 0 & 0 & 0 \\ -\rho_2 & 0 & 1 & 0 & 0 & 0 & 0 & 0 & 0 & 0 & 0 & 0 \\ 0 & 0 & 0 & 0 & 0 & 0 & 0 & 0 & 0 & 0 & 0 & 0 \\ 0 & 0 & 0 & 0 & 0 & 0 & 0 & 0 & 0 & 0 & 0 & 0 \\ 0 & 0 & 0 & 0 & 0 & 0 & 0 & 0 & 0 & 0 & 0 & 0 \\ 0 & 0 & 0 & 0 & 0 & 0 & 1 & -\rho_3 & \rho_2 & 0 & 0 & 0 \\ 0 & 0 & 0 & 0 & 0 & 0 & \rho_3 & 1 & 0 & 0 & 0 & 0 \\ 0 & 0 & 0 & 0 & 0 & 0 & -\rho_2 & 0 & 1 & 0 & 0 & 0 \\ 0 & 0 & 0 & 0 & 0 & 0 & 0 & 0 & 0 & 0 & 0 & 0 \\ 0 & 0 & 0 & 0 & 0 & 0 & 0 & 0 & 0 & 0 & 0 & 0 \\ 0 & 0 & 0 & 0 & 0 & 0 & 0 & 0 & 0 & 0 & 0 & 0 \end{bmatrix} \quad \begin{bmatrix} \bar{F}_1 \\ \bar{F}_2 \\ \bar{F}_3 \\ \bar{F}_4 \\ \bar{F}_5 \\ \bar{F}_6 \\ \bar{F}_7 \\ \bar{F}_8 \\ \bar{F}_9 \\ \bar{F}_{10} \\ \bar{F}_{11} \\ \bar{F}_{12} \end{bmatrix}$$

$$\{\bar{F}'\} = [B'] \{\bar{F}\} \tag{26}$$

Equation (26) when used to evaluate the matrix $[\Delta B]$ will result in an unsymmetric co-efficient matrix when the term $([\Delta B] \{S\})$ is expressed in terms of the vector $\{\Delta\bar{u}\}$. To restore symmetry; in evaluating $[\Delta B]$ we take into account the change in length of the member and that the moments producing shear are constant rather than the transverse nodal forces. If S_o is the initial transverse force; and ΔS_o its variation,

$$(S_o + S_o)(\ell + \delta) = S_o \ell$$

$$\therefore \quad S_o = -\frac{S_o \delta}{\ell} \; ; \quad \text{ignoring 2nd order terms}$$

where

$$\delta = \Delta\bar{u}_7 - \Delta\bar{u}_1$$

$\{\Delta\bar{F}_{\sim u}\}$ which is the change in the vector $\{\bar{F}_{\sim}\}$ resulting from the variation $\{\Delta\bar{u}_{\sim}\}$ is thus

$$\{\Delta\bar{F}_{\sim u}\} = \{\bar{F}_{\sim}'\} - \{\bar{F}_{\sim}\}$$

$$\begin{bmatrix} \Delta\bar{F}_1 \\ \Delta\bar{F}_2 \\ \Delta\bar{F}_3 \\ \Delta\bar{F}_4 \\ \Delta\bar{F}_5 \\ \Delta\bar{F}_6 \\ \Delta\bar{F}_7 \\ \Delta\bar{F}_8 \\ \Delta\bar{F}_9 \\ \Delta\bar{F}_{10} \\ \Delta\bar{F}_{11} \\ \Delta\bar{F}_{12} \end{bmatrix} = \begin{bmatrix} 0 & -\rho_3 & \rho_2 & 0 & 0 & 0 & 0 & 0 & 0 & 0 & 0 & 0 \\ \rho_3 & -\delta/\ell & 0 & 0 & 0 & 0 & 0 & 0 & 0 & 0 & 0 & 0 \\ -\rho_2 & 0 & -\delta/\ell & 0 & 0 & 0 & 0 & 0 & 0 & 0 & 0 & 0 \\ 0 & 0 & 0 & 0 & 0 & 0 & 0 & 0 & 0 & 0 & 0 & 0 \\ 0 & 0 & 0 & 0 & 0 & 0 & 0 & 0 & 0 & 0 & 0 & 0 \\ 0 & 0 & 0 & 0 & 0 & 0 & 0 & 0 & 0 & 0 & 0 & 0 \\ 0 & 0 & 0 & 0 & 0 & 0 & 0 & -\rho_3 & \rho_2 & 0 & 0 & 0 \\ 0 & 0 & 0 & 0 & 0 & 0 & \rho_3 & -\delta/\ell & 0 & 0 & 0 & 0 \\ 0 & 0 & 0 & 0 & 0 & 0 & -\rho_2 & 0 & -\delta/\ell & 0 & 0 & 0 \\ 0 & 0 & 0 & 0 & 0 & 0 & 0 & 0 & 0 & 0 & 0 & 0 \\ 0 & 0 & 0 & 0 & 0 & 0 & 0 & 0 & 0 & 0 & 0 & 0 \\ 0 & 0 & 0 & 0 & 0 & 0 & 0 & 0 & 0 & 0 & 0 & 0 \end{bmatrix} \begin{bmatrix} \bar{F}_1 \\ \bar{F}_2 \\ \bar{F}_3 \\ \bar{F}_4 \\ \bar{F}_5 \\ \bar{F}_6 \\ \bar{F}_7 \\ \bar{F}_8 \\ \bar{F}_9 \\ \bar{F}_{10} \\ \bar{F}_{11} \\ \bar{F}_{12} \end{bmatrix}$$

$$= \begin{bmatrix} \frac{-\rho_3}{\ell} & \frac{-\rho_3}{\ell} & \frac{-\rho_2}{\ell} & \frac{-\rho_2}{\ell} & 0 & 0 \\ \frac{-\delta}{\ell^2} & \frac{-\delta}{\ell^2} & 0 & 0 & 0 & -\rho_3 \\ 0 & 0 & \frac{\delta}{\ell^2} & \frac{\delta}{\ell^2} & 0 & \rho_2 \\ 0 & 0 & 0 & 0 & 0 & 0 \\ 0 & 0 & 0 & 0 & 0 & 0 \\ 0 & 0 & 0 & 0 & 0 & 0 \\ \frac{\rho_3}{\ell} & \frac{\rho_3}{\ell} & \frac{\rho_2}{\ell} & \frac{\rho_2}{\ell} & 0 & 0 \\ \frac{\delta}{\ell^2} & \frac{\delta}{\ell^2} & 0 & 0 & 0 & \rho_3 \\ 0 & 0 & \frac{-\delta}{\ell^2} & \frac{-\delta}{\ell^2} & 0 & -\rho_2 \\ 0 & 0 & 0 & 0 & 0 & 0 \\ 0 & 0 & 0 & 0 & 0 & 0 \\ 0 & 0 & 0 & 0 & 0 & 0 \end{bmatrix} \begin{bmatrix} M_{13} \\ M_{23} \\ M_{12} \\ M_{22} \\ M_t \\ P \end{bmatrix}$$

$$= [\underset{\sim}{\Delta B}] \{\underset{\sim}{S}\}$$

$$
= \begin{bmatrix}
0 & \frac{M_{13}+M_{23}}{\ell^2} & -\frac{M_{12}+M_{22}}{\ell^2} & 0 & 0 & 0 & 0 & -\frac{M_{13}+M_{23}}{\ell^2} & \frac{M_{12}+M_{22}}{\ell^2} & 0 & 0 & 0 \\
 & \frac{P}{\ell} & 0 & 0 & 0 & 0 & -\frac{M_{13}+M_{23}}{\ell^2} & -\frac{P}{\ell} & 0 & 0 & 0 & 0 \\
 & & \frac{P}{\ell} & 0 & 0 & 0 & \frac{M_{12}+M_{22}}{\ell^2} & 0 & -\frac{P}{\ell} & 0 & 0 & 0 \\
 & & & 0 & 0 & 0 & 0 & 0 & 0 & 0 & 0 & 0 \\
 & & & & 0 & 0 & 0 & 0 & 0 & 0 & 0 & 0 \\
 & & & & & 0 & 0 & 0 & 0 & 0 & 0 & 0 \\
 & & & & & & 0 & \frac{M_{13}+M_{23}}{\ell^2} & -\frac{M_{12}+M_{22}}{\ell^2} & 0 & 0 & 0 \\
 & & & & & & & \frac{P}{\ell} & 0 & 0 & 0 & 0 \\
\text{Symmetry} & & & & & & & & \frac{P}{\ell} & 0 & 0 & 0 \\
 & & & & & & & & & 0 & 0 & 0 \\
 & & & & & & & & & & 0 & 0 \\
 & & & & & & & & & & & 0
\end{bmatrix}
\begin{bmatrix} \Delta\bar{u}_1 \\ \Delta\bar{u}_2 \\ \Delta\bar{u}_3 \\ \Delta\bar{u}_4 \\ \Delta\bar{u}_5 \\ \Delta\bar{u}_6 \\ \Delta\bar{u}_7 \\ \Delta\bar{u}_8 \\ \Delta\bar{u}_9 \\ \Delta\bar{u}_{10} \\ \Delta\bar{u}_{11} \\ \Delta\bar{u}_{12} \end{bmatrix}
$$

$$
= \underset{\sim}{[N]}\ \{\Delta\bar{\underset{\sim}{u}}\} \qquad (27)
$$

Substituting Equations (21), (23) and (27) into (25), the incremental equilibrium equation in member co-ordinates are

$$
\{\Delta\bar{\underset{\sim}{F}}\} = \underset{\sim}{[B]}\ \underset{\sim}{\{K\}}\ [\Delta\underset{\sim}{V}] + \underset{\sim}{[N]}\ \{\Delta\bar{\underset{\sim}{u}}\}
$$

$$
= (\underset{\sim}{[B]}\ \underset{\sim}{[K]}\ \underset{\sim}{[B]}^T + \underset{\sim}{[N]})\ \{\Delta\bar{\underset{\sim}{u}}\}
$$

$$
= \underset{\sim}{[\bar{K}]}\ \{\Delta\bar{u}\} \qquad (28)
$$

2.2.3 Transformation from Member Co-ordinates to Global Co-Ordinates

The member orientation matrix, which is the direction cosines of the member axes with respect to the global co-ordinates X_1, X_2 and X_3 is denoted by $[\underset{\sim}{r}]$. Let

$$[\underset{\sim}{R}] = \begin{bmatrix} [\underset{\sim}{r}] & 0 & 0 & 0 \\ 0 & [\underset{\sim}{r}] & 0 & 0 \\ 0 & 0 & [\underset{\sim}{r}] & 0 \\ 0 & 0 & 0 & [\underset{\sim}{r}] \end{bmatrix}$$

We thus have

$$\{\Delta\underset{\sim}{F}\} = [\underset{\sim}{R}]\ \{\Delta\bar{\underset{\sim}{F}}\} \tag{29}$$

and by contragredience,

$$\{\Delta\bar{\underset{\sim}{u}}\} = [\underset{\sim}{R}]^T\ \{\Delta\underset{\sim}{u}\} \tag{30}$$

Substituting Equation (28) into (29)

$$\begin{aligned} \{\Delta\underset{\sim}{F}\} &= [\underset{\sim}{R}]\ [\bar{\underset{\sim}{K}}]\ \{\Delta\bar{\underset{\sim}{u}}\} \\ &= [\underset{\sim}{R}]\ [\bar{\underset{\sim}{K}}]\ [\underset{\sim}{R}^T]\ \{\Delta\underset{\sim}{u}\} \\ &= [\underset{\sim}{K}_G]\ \{\Delta\underset{\sim}{u}\} \end{aligned} \tag{31}$$

which is the incremental equilibrium equation in global co-ordinates.

2.2.4 Evaluation of Member Rotational Deformations from Joint Orientation Matrix

The 'joint orientation matrix', $[\underset{\sim}{\alpha}]$ is initially assumed to be parallel to the global axes. The incremental rotation matrix for a joint in global co-ordinates is

$$[\underset{\sim}{\Delta\Omega}] = \begin{bmatrix} 0 & -\Delta\Omega_3 & \Delta\Omega_2 \\ \Delta\Omega_3 & 0 & -\Delta\Omega_1 \\ -\Delta\Omega_2 & \Delta\Omega_1 & 0 \end{bmatrix} \tag{32}$$

where $\Delta\Omega_1 = \Delta u_4$, $\Delta\Omega_2 = \Delta u_5$, $\Delta\Omega_3 = \Delta u_6$ for joint (1)

and $\Delta\Omega_1 = \Delta u_{10}$, $\Delta\Omega_2 = \Delta u_{11}$, $\Delta\Omega_3 = \Delta u_{12}$ for joint (2)

This results in an increment in the joint orientation matrix which is

$$[\underset{\sim}{\Delta\alpha}] = [\underset{\sim}{\Delta\Omega}]\,[\underset{\sim}{\alpha}] \tag{33}$$

and thus the updated joint orientation matrix, $[\underset{\sim}{\alpha}] + [\underset{\sim}{\Delta\alpha}]$ can be evaluated.

The two end sections of the member will in general be not parallel to each other. 'End section orientation matrices' are thus defined to describe them with the matrices $\left[p^{(1)}\right]$ and $\left[p^{(2)}\right]$ for end section (1) and (2) respectively. They are related to the joint orientation matrices by

$$[\underset{\sim}{p}] = [\underset{\sim}{\alpha}]\left[\underset{\sim}{r}^{(0)}\right] \tag{34}$$

where $\left[\underset{\sim}{r}^{(o)}\right]$ = member orientation matrix in undeformed configuration.

The first column of the member orientation matrix, $[\underset{\sim}{r}]$ represents the vector of direction cosines of the member chord (the line joining the end sections). This can be obtained from the global translational displacements of the nodes. Denoting the first column of $[\underset{\sim}{r}]$ by $[\underset{\sim 1}{r}]$, the following relation applies for the case of small relative rotations of the member.

$$\left\{\begin{array}{c} 1 \\ -\theta_{13} \\ \theta_{12} \end{array}\right\} = \left[\underset{\sim}{p}^{(1)}\right]^T \{\underset{\sim 1}{r}\}$$

$$\left\{\begin{array}{c} 1 \\ -\theta_{23} \\ \theta_{22} \end{array}\right\} = \left[\underset{\sim}{p}^{(2)}\right] \{\underset{\sim 1}{r}\} \qquad (35)$$

and

$$\theta_t = -\left\{\underset{\sim 2}{p}^{(1)}\right\}^T \left\{\underset{\sim 3}{p}^{(2)}\right\} = \left\{\underset{\sim 3}{p}^{(1)}\right\}^T \left\{\underset{\sim 2}{p}^{(2)}\right\}$$

where $\left\{p_j^{(i)}\right\}$ = j column of the end orientation matrix of joint i.

To evaluate the second and third columns of $[\underset{\sim}{r}]_1$, which represents the vector of direction cosines of the 2 member principal directions, let us define the following incremental rotation matrix for the two end sections.

$$\left[\underset{\sim}{e}^{(1)}\right] = \begin{bmatrix} 1 & \theta_{13} & -\theta_{12} \\ -\theta_{13} & 1 & 0 \\ \theta_{12} & 0 & 1 \end{bmatrix}$$

$$\left[\underset{\sim}{e}^{(2)}\right] = \begin{bmatrix} 1 & \theta_{23} & -\theta_{22} \\ -\theta_{23} & 1 & 0 \\ \theta_{22} & 0 & 1 \end{bmatrix} \qquad (36)$$

Due to the member relative rotations, the new end section orientation matrices will be $\left[p^{(1)}\right]\left[e^{(1)}\right]$ and $\left[p^{(2)}\right]\left[e^{(2)}\right]$. The member x_2 and x_3 axes could then be defined as the principal direction of an average cross-section, hence

$$[\underset{\sim}{r}] = \frac{1}{2}\left[\underset{\sim}{p}^{(1)}\right]\left[\underset{\sim}{e}^{(1)}\right] + \frac{1}{2}\left[\underset{\sim}{p}^{(2)}\right]\left[\underset{\sim}{e}^{(2)}\right] \qquad (37)$$

3. SOLUTION STRATEGIES FOR TRAVERSING LIMIT POINTS

One of the earliest techniques developed was to introduce spring coefficients into the incremental stiffness matrix [31,32]. This has the effect of augmenting the stiffness matrix so that it remains positive definite throughout the entire range of the analysis. This augmentation is achieved by adding to the structural stiffness matrix $[\underset{\sim}{K}]$ by the following matrix of rank one;

$$[\underset{\sim}{K}_A] = \frac{k}{\theta^2}\{\underset{\sim}{Q}\}\{\underset{\sim}{Q}\}^T \qquad (38)$$

where k = given stiffness of a fictitious elastic spring.

$\{\underset{\sim}{Q}\}$ = reference load vector.

θ = the norm of the matrix $[\underset{\sim}{K}]$.

The augmented equilibrium equations are thus

$$[\underset{\sim}{K} + \underset{\sim}{K}_A]\ \{\underset{\sim}{r}\} = \{\underset{\sim}{P}\} \tag{39}$$

where $\{\underset{\sim}{P}\}$ = total external load of augmented system, and the load reduction factor, Λ applied to $\{\underset{\sim}{P}\}$ to obtain the actual external load is

$$\Lambda = 1 - \frac{k}{\theta^2}\ \{\underset{\sim}{Q}\}^T\ \{\underset{\sim}{r}\} \tag{40}$$

which can be computed once Equation (39) is solved for $\{\underset{\sim}{r}\}$. For the case of simple load and one spring, as illustrated in Figure 4, this method is easy to apply. However, this technique cannot be easily justified from a mathematical viewpoint when multiple springs are added. In addition, for a multi degree of freedom system, the coupling of the artificial stiffness may destroy the banded nature of the stiffness matrix. Also the reference stiffness of the applied springs have to be obtained by trial and it should not be used for structures with local buckling or a tendency to bifurcate.

Due to the singularity of the incremental stiffness matrix at the extremum points, equilibrium iterations easily break down. To overcome this problem which has plagued earlier researchers employing an incremental-iterative solution strategy, Bergan [24,25,33] introduced the concept of a current stiffness parameter, S_p. With reference to Figure 5, S_p is defined as

$$S_p = \frac{\left(\frac{dp}{dr}\right)_i}{\left(\frac{dp}{dr}\right)_o} \tag{41}$$

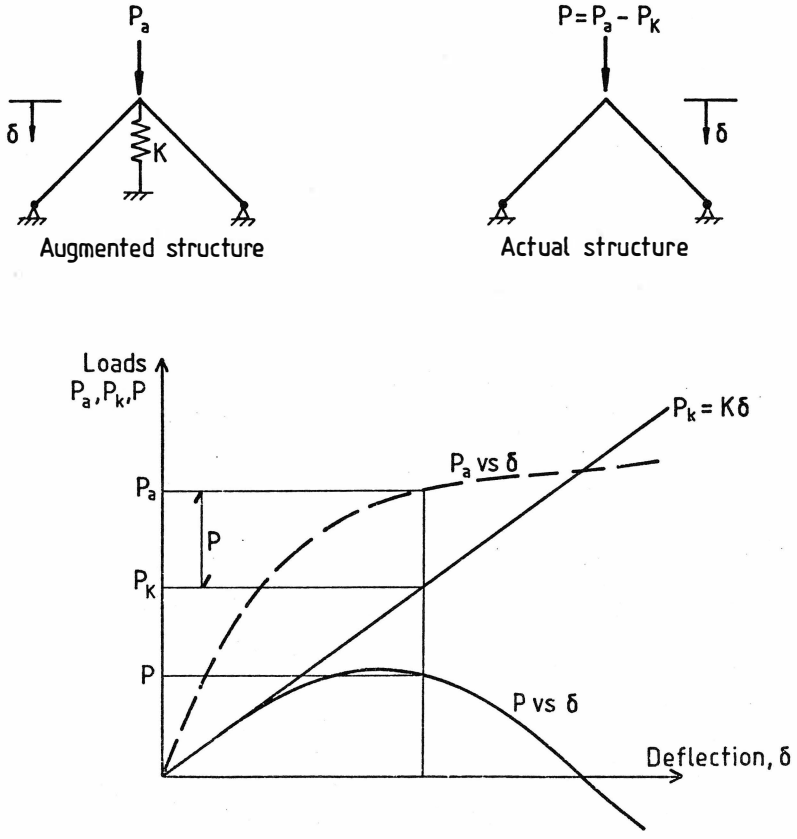

Figure 4. Spring Constant Method

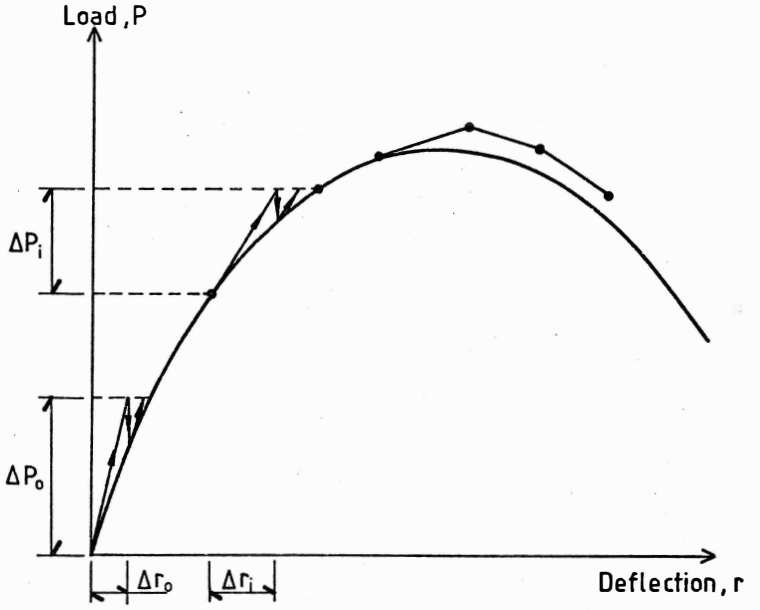

Figure 5. 'Current Stiffness Parameter' Method

with $\frac{dp}{dr} = \frac{\Delta p_i}{\Delta \underset{\sim}{r}^T \underset{\sim}{R}_c}$,

$\underset{\sim}{R}_c$ = characteristic load, which is chosen to be the reference load vector, $\underset{\sim}{R}$ ref.

Now, $\Delta \underset{\sim}{R}_i$ = incremental external load

$= \Delta p_i \underset{\sim}{R}$ ref.

$\therefore \quad S_p = \frac{\Delta p_i \ \Delta p_i}{\Delta \underset{\sim}{r}_i^T \Delta \underset{\sim}{R}_i} \ \frac{\Delta \underset{\sim}{r}_o^T \Delta \underset{\sim}{R}_o}{\Delta p_o \ \Delta p_o}$

$$= \left(\frac{\Delta p_i}{\Delta p_o}\right)^2 \frac{\Delta \underset{\sim}{r}_o^T \underset{\sim}{K}_o \Delta \underset{\sim}{r}_o}{\Delta \underset{\sim}{r}_i^T \underset{\sim}{K}_i \Delta \underset{\sim}{r}_i} \tag{42}$$

The current stiffness parameter has an initial value of 1.0 and is zero at a singular point. This parameter can thus sense in advance the approach of an instability, and by suppressing equilibrium iterations when the magnitude of this parameter is less than a threshold value, the solution is prevented from breaking down. The solution, by pure load incrementation, is then made to 'jump' over the limit point and advance along its path. On the negative definite portion of the solution path, the 'current stiffness parameter' is negative and when this occurs the algorithm reverses the load and displacement increments. The solution then proceeds with negative load increments until the next extremum point is reached. Due to the low stiffness at the limit points, the load increment can produce uncontrolled displacements which may cause the solution to diverge. Small load increments are thus necessary, and this also helps to prevent drifting away from the equilibrium path. Even with small increments, the displacement can still be too large; and a simple method to prevent this is to calculate a norm of the displacement increment and scale back both load and displacement increments according to how much a specified maximum value has been exceeded.

A popular method for avoiding the singularities is to increment the load parameter to the limit point, solving for displacements, then on beyond this point by incrementing a characteristic displacement to evaluate the corresponding load parameter. This was first described by Argyris [34], but unfortunately his approach led to a system of non-symmetric equations. Alternative approaches were presented by Pian and Tong [35], Yamada [36] and Zienkiewicz [37] which circumvented the non-symmetric matrix problem, but were applicable only for a step-by-step

procedure without iterating to equilibrium within the displacement increment. These also required a modification to the incremental stiffness matrix. A scheme suggested by Haisler and Stricklin [38], which makes use of an initial value formulation, allows one to iterate to convergence. The proposed computational procedure is, however, cumbersome and a simpler procedure as described by Batoz and Dhatt [39] exists.

In the algorithm presented by Batoz and Dhatt, the tangent stiffness matrix $\underset{\sim}{K}$ is used to complete $\Delta\underset{\sim}{u}_r$ which is the incremental displacement due to the residual forces, $\underset{\sim}{R}$ and also $\Delta\underset{\sim}{u}_e$ which is that due to an arbitrary external load increment $\underset{\sim}{P}$ i.e.

$$\Delta\underset{\sim}{u}_r = \underset{\sim}{K}^{-1}\,\underset{\sim}{R}$$

$$\Delta\underset{\sim}{u}_e = \underset{\sim}{K}^{-1}\,\underset{\sim}{P} \tag{43}$$

The actual external load applied is $\Delta\lambda\underset{\sim}{P}$ and this factor is obtained by specifying that the displacement increment at degree of freedom, n, satisfies a displacement, δ, where

$$\delta = \Delta\underset{\sim}{u}_r^{(n)} + \Delta\lambda\Delta\underset{\sim}{u}_e^{(n)} \tag{44}$$

The actual incremental displacement vector, $\Delta\underset{\sim}{u}$ is then given by

$$\Delta\underset{\sim}{u} = \Delta\underset{\sim}{u}_r + \Delta\lambda\Delta\underset{\sim}{u}_e \tag{45}$$

The above procedure enables one to obtain the increment at the beginning of the iteration sequence. Subsequent iterations are performed in exactly the same manner except that δ is now specified to be zero; iterating to convergence is achieved through keeping the selected nodal

displacement constant. This particular strategy, in a more generalised form was also described by Powell and Simons [40].

From the writers' experience with the above strategy, it has proved to be both stable and efficient. However, it has the distinct disadvantage that the displacement component at the degree of freedom chosen to control the incrementation has to be monotically increasing. If the controlling displacement snaps back from one load level to another, the strategy will fail to converge. A proper choice of the controlling displacement is thus essential and for some structures this is not obvious and some experimentation will be necessary.

It has been observed that instead of using a single component of the displacement vector, it is possible to use some measure of the complete vector as the controlling parameter. This is the path followed by Riks [41] and Wempner [42] where the load step, $\Delta\lambda$, is limited by the following constraint equation.

$$\Delta\underset{\sim}{u}^T.\Delta\underset{\sim}{u} + \Delta\lambda^2\Delta\underset{\sim}{P}^T.\Delta\underset{\sim}{P} = \Delta\ell^2 \qquad (46)$$

In the equation, $\Delta\ell$ is a prescribed scalar which fixes the length of the increment. This constraint equation was originally added to the incremental stiffness expression but this unfortunately destroys the bandedness and symmetry of the stiffness matrix. By adopting a two step technique used by Batoz and Dhatt, as described above, this problem can be overcome. This modified 'constant arc length' strategy of Riks and Wempner is presented by Ramm in Reference [26]; where both iteration in a 'plane' normal to the tangent and iteration in a 'sphere' are described. This is illustrated in Figure 6. In the work of Crisfield [43], instead of applying the constraint equation of (46), use was made of the following constraint.

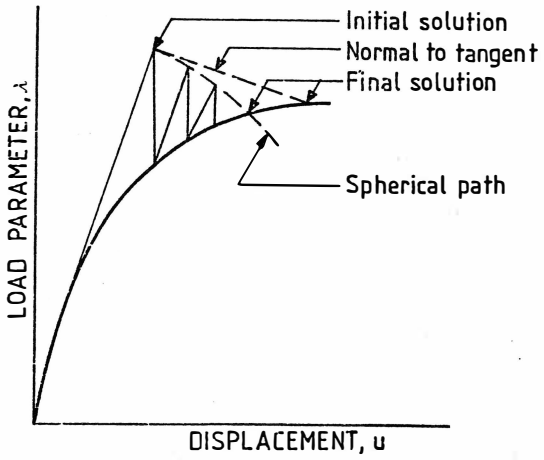

Figure 6. Rik's method with iteration about a 'sphere' or iteration about a 'normal plane'

$$\Delta \underset{\sim}{u}^{T} . \Delta \underset{\sim}{u} = \Delta \ell^2 \qquad (47)$$

which from his experience appears to be numerically better. The 'constant arc length' method, by generalising the constraint equation from that for a single component of the displacement vector to that for the scalar product of the vector, is thus able to overcome the problem of the choice of a monotonically increasing displacement component associated with the single displacement component control techniques. Equilibrium iterations near a singularity do not pose any particular problems, as is the case with the 'current stiffness parameter' of Bergan. By iterating about a constant arc length or a constant displacement component as in the Batoz and Dhatt strategy, we are iterating in the external load space as well as in the displacement space, and this is more efficient than conventional Newton-type strategies at constant load. This point is illustrated by the work of Crisfield in Reference [43]. From this brief review, the writers conclude that in terms of generality,

effectiveness and robustness, the 'constant arc length' method is superior to the other described strategies.

4. CONSTANT ARC LENGTH STRATEGY OF CRISFIELD

At the start of an arc length increment, $\Delta \underset{\sim}{u}^{(o)}$ is the incremental displacement vector, $\Delta\lambda^{(o)}$ the corresponding load multiplier and $\Delta\ell$ the prescribed generalised arc length. Application of the arc length constraint results in

$$\Delta \underset{\sim}{u}^{(o)T} . \Delta \underset{\sim}{u}^{(o)} = \Delta\ell^2 \tag{48}$$

with

$$\Delta \underset{\sim}{u}^{(o)} = \underset{\sim}{K}^{-1} \left(\Delta\lambda^{(o)} \underset{\sim}{P} \right) \tag{49}$$

$\underset{\sim}{K}$ = the incremental stiffness matrix, and $\underset{\sim}{P}$ = an arbitrary external load vector. Solving (48) and (49) will then yield $\Delta\lambda^{o}$. In the paper of Crisfield [43] and Ramm [26], it was suggested that the sign of $\Delta\lambda^{o}$ should follow that of the previous increment unless the sign of the determinant of the incremental stiffness matrix has changed. From the examples presented by them, this criterion appears to be satisfactory. However, in the case of structures exhibiting multiple negative eigenvalues behaviour, this simple criterion does not always work and it appears better to base the sign change on that of the sign of the incremental work done, ΔW where

$$\Delta W = \Delta \underset{\sim}{u}^{(o)T} . \underset{\sim}{P} \tag{50}$$

If the sign of W has changed from that of the previous increment, the sign of $\Delta\lambda^{(o)}$ is reversed from that of its previous value.

After the initial increment, the displacement is then iterated to convergence. At the i th iteration

$$\Delta \underset{\sim}{u}_e^{(i)} = \underset{\sim}{K}^{-1} \underset{\sim}{P} \tag{51}$$

and

$$\Delta \underset{\sim}{u}_r^{(i)} = \underset{\sim}{K}^{-1} \underset{\sim}{R}^{(i-1)} \tag{52}$$

where $\Delta \underset{\sim}{u}_e^{(i)}$ = displacement increment due to the arbitrary external load, $\Delta \underset{\sim}{u}_r^{(i)}$ = displacement increment due to the residual force vector, $\underset{\sim}{R}^{(i-1)}$ at the end of the (i-1) th iteration. In the Newton-Raphson method the matrix $\underset{\sim}{K}$ is reformed after every iteration, while in the modified Newton-Raphson iterative scheme it remains constant or is reformed after a number of iterations. If $\underset{\sim}{K}$ is constant, then so also is $\Delta \underset{\sim}{u}_e^{(i)}$ throughout the increment and there is thus no need to recalculate it at every iteration. At the i th iteration, the iterative displacement, $\Delta \underset{\sim}{u}^{(i)}$, is

$$\Delta \underset{\sim}{u}^{(i)} = \Delta\lambda^{(i)} \Delta \underset{\sim}{u}_e^{(i)} + \Delta \underset{\sim}{u}_r^{(i)} \tag{53}$$

and the incremental displacement up to the i th iteration, $\delta \underset{\sim}{u}^{(i)}$ is

$$\delta \underset{\sim}{u}^{(i)} = \delta \underset{\sim}{u}^{(i-1)} + \Delta \underset{\sim}{u}^{(i)} \tag{54}$$

This incremental displacement is made to satisfy the arc length constraint of Equation (48) and thus

$$\delta\underset{\sim}{u}^{(i)T}.\delta\underset{\sim}{u}^{(i)} = \Delta\ell^2$$

$$\left(\delta\underset{\sim}{u}^{(i-1)} + \Delta\underset{\sim}{u}^{(i)}\right)^T.\left(\delta\underset{\sim}{u}^{(i-1)} + \Delta\underset{\sim}{u}^{(i)}\right) = \Delta\ell^2$$

$$\left(\delta\underset{\sim}{u}^{(i-1)} + \Delta\lambda^{(i)}\,\Delta\underset{\sim}{u}_e^{(i)}\right)^T.\left(\delta\underset{\sim}{u}^{(i-1)} + \Delta\lambda^{(i)}\,\Delta\underset{\sim}{u}_e^{(i)} + \Delta\underset{\sim}{u}_r^{(i)}\right) = \Delta\ell^2 \qquad (55)$$

which leads to the following quadratic

$$a_1\left[\Delta\lambda^{(i)}\right] + a_2\left[\Delta\lambda^{(i)}\right] + a_3 = 0$$

where

$$a_1 = \Delta\underset{\sim}{u}_e^{(i)T}.\Delta\underset{\sim}{u}_e^{(i)}$$

$$a_2 = 2\left(\delta\underset{\sim}{u}^{(i-1)} + \Delta\underset{\sim}{u}_r^{(i)}\right)^T.\Delta\underset{\sim}{u}_e^{(i)}$$

$$a_3 = \left(\delta\underset{\sim}{u}^{(i-1)} + \Delta\underset{\sim}{u}_r^{(i)}\right)^T.\left(\delta\underset{\sim}{u}^{(i-1)} + \Delta\underset{\sim}{u}_r^{(i)}\right) - \Delta\ell^2 \qquad (56)$$

Two values of $\Delta\lambda^{(i)}$ are possible and to void 'doubling-back' the solution path, the correct choice of $\Delta\lambda^{(i)}$ is that in which the scalar product of the incremental displacement vector, $\delta\underset{\sim}{u}^{(i-1)}$ is a positive quantity. In the event that both choices of $\Delta\lambda^{(i)}$ yield a positive result, the correct root is the one nearest to the linear solution.

$$\Delta\lambda^{(i)} = a_3/a_2 \qquad (57)$$

The success of this nonlinear solution strategy depends on the quadratic of Equation (56) yielding real roots. Imaginary roots will occur if

$$a_2^2 - 4a_1 a_3 < 0 \tag{58}$$

and this will indeed be so if a norm measure of $\Delta\underset{\sim}{u}_r^{(i)}$ is much larger than that of $\Delta\underset{\sim}{u}_e^{(i)}$. This will happen if the stiffness in the direction of the degree of freedoms not acted on by the external force vector become very small relative to that of the degree of freedoms carrying the external loads. In the majority of cases, this is unlikely to occur, and from the writers' experience this will probably occur only in structures exhibiting multiple instability directions at a point. A structure showing this type of behaviour is described in the numerical examples.

5. EVALUATION OF POST-BIFURCATION EQUILIBRIUM PATH (SECONDARY PATH)

To investigate the stability of an equilibrium configuration it is necessary to formulate the quadratic form

$$\frac{\partial^2 V}{\partial q_i \partial q_j} \delta q_i \, \delta q_j = V_{ij} \, \delta q_i \, q_j \tag{59}$$

where

V = potential energy of the system.

q = generalised co-ordinates

V_{ij} = coefficient matrix of the quadratic form which is equivalent to the incremental stiffness matrix, $\underset{\sim}{K}$ defined above.

According to the theory of stability of conservative systems, the stability of the equilibrium state is ensured if the above quadratic form is positive definite. Equation (59) is indefinite for an unstable configuration while the transition between a stable and an unstable point of the equilibrium path is denoted by a positive semi-definite Equation (59). The critical equilibrium state is in general either a limit point or a bifurcation point and they are illustrated in Figure 7. A necessary but not sufficient condition for the existence of a critical state is the vanishing of the determinent of the incremental stiffness matrix.

$$\det\left|V_{ij}\right| = \det|\underset{\sim}{K}| = 0 \tag{60}$$

This can be easily obtained during the factorisation of the tangent stiffness matrix in the incremental-iterative solution strategy, since it is the product of all terms of the diagonal matrix in the $L\ D\ L^T$ decomposition. The precise definition of a critical equilibrium state is given by the solution of the following eigenvalue problem

$$\left[V_{ij} - \Omega(k)\ \delta_{ij}\right] a_j(k) = 0 \tag{61}$$

where a(k) denote the eigenvector and $\Omega(k)$ the eigenvalues which define the critical states. A limit point is distinguished from a bifurcation point in that it is characterised by a vanishing load increase.

The incremental-iterative solution strategy described in the sections above is capable of continuing the computation of the fundamental (basic) equilibrium path beyond the critical points. However, to follow a secondary path after a bifurcation point, will require a modification to the described solution strategy at the arc length increment immediately after the bifurcation point. The vector $\underset{\sim}{r}_F$

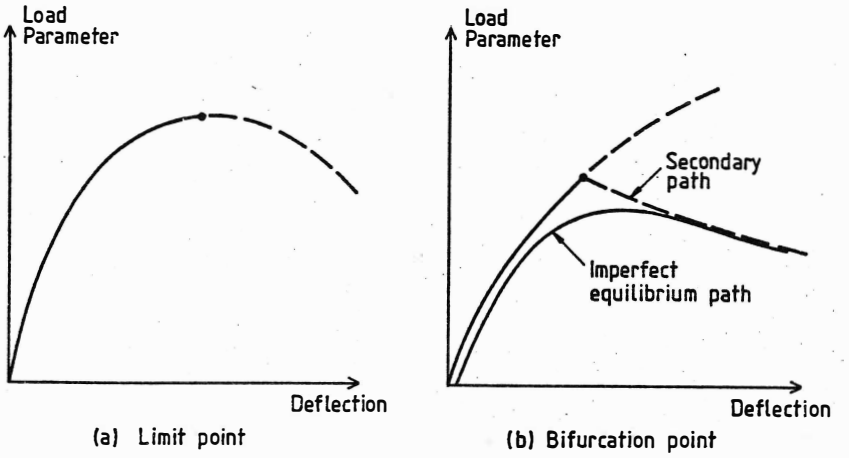

Figure 7. Critical points

tangential to the fundamental path at the bifurcation point, B can be calculated approximately as

$$\underset{\sim}{r}_F = \frac{1}{2}\left(\Delta\underset{\sim}{q}^m + \Delta\underset{\sim}{q}^{m+1}\right) \tag{62}$$

where $\Delta\underset{\sim}{q}^m$ = incremental generalised displacement vector at point m. The unit vector $\underset{\sim}{t}_F$, colinear with $\underset{\sim}{r}_F$ is thus

$$\underset{\sim}{t}_F = \frac{\underset{\sim}{r}_F}{\left(\underset{\sim}{r}_F^T \cdot \underset{\sim}{r}_F\right)^{\frac{1}{2}}} \tag{63}$$

According to References [41 and 44] the vector $\underset{\sim}{t}_B$ tangential to the secondary post bifurcation path at B is given by

$$\underset{\sim}{t}_B = \alpha\{\underset{\sim}{a} + \mu\underset{\sim}{t}_F\}$$

$$\alpha = \left|\left\{\underset{\sim}{a} + \mu\underset{\sim}{t}_F\right\}^T \left\{\underset{\sim}{a} + \mu\underset{\sim}{t}_F\right\}\right|^{-\frac{1}{2}} \tag{64}$$

where $\underset{\sim}{a}$ = eigenvector of the incremental stiffness matrix, $\underset{\sim}{K}$ and the coefficient μ is a function of the third derivative of the potential energy [41]. This evaluation of the third derivative is difficult and thus an approximation to $\underset{\sim}{t}_B$ such that the approximation, $\underset{\sim}{t}_B^{(i)}$ is orthogonal to $\underset{\sim}{t}_F$ is used. Therefore

$$\mu = -\underset{\sim}{a}^T \underset{\sim}{t}_F \tag{65}$$

The displacement increment for the first iteration of the arc length increment after the critical point, $\underset{\sim}{q}_C$ can be assumed to be

$$\Delta\underset{\sim}{q}_B^{(1)} = \underset{\sim}{t}_B^{(1)} \Delta\ell \tag{66}$$

where $\Delta\ell$ = prescribed generalised arc length.

Iteration to equilibrium is then performed as described in Section 4, with the modification that the incremental stiffness matrix used is $\underset{\sim}{K}\left(\underset{\sim}{q}_C + \underset{\sim}{q}_B\right)$ to prevent the solution from coming back to the fundamental equilibrium path. This described technique of superimposing a fraction of the eigenmode on the displacement field at the bifurcation point can be called the 'perfect approach'.

A simpler alternative without the need to compute the eigenvectors will be to impose either a small perturbation in load or geometry to the structure. This 'imperfect approach' will yield a load-deflection path which approaches the perfect post-bifurcation path with increased

deformation of the structure (see Figure 7).

6. EXTRAPOLATED STIFFNESS PROCEDURE

Let us consider the efficiency of the linearised incremental-iterative arc length technique. It is apparent from Figure 8 that for the one degree of freedom cases, the point (a) which is the result after the first iteration, is a poor guess of the final solution. If instead of using the gradient to the solution path at the beginning of the arc length increment, it is possible to use the gradient of the point half arc length ahead, it would appear that the result after the first iteration will give a much better estimate to the final solution. This is illustrated in Figure 8 where m is midway along the arc a-b. For a multi degree of freedom system, by using the tangent stiffness half an arc length ahead instead of the value at the beginning of the increment, the same conclusion should apply.

The pertinent question now is; how to obtain the tangent stiffness half an arc length ahead since the nodal displacement associated with the point are not known at the beginning of the increment. For the strategy proposed herein, this is achieved by extrapolating forward the tangent stiffness from previous arc length increments. A 3 point Lagrange interpolation polynominal [45] will be used and thus in addition to the tangent stiffness at the beginning of the arc length increment, its value at the previous two increments must be retained. The tangent stiffness matrices are stored in 'skyline' linear arrays. Let k_j, k_{j-1} and k_{j-1} represent and element of the tangent stiffness at the beginning of the j, (j-1) and (j-2) increment respectively. k_j is the corresponding element of the extrapolated tangent stiffness half an arc length ahead at the j th increment and it is given by

$$k'_j = \frac{(2.5 - 1)\,(2.5 - 2)}{(0 - 1)\,(0 - 2)}\,k_{j-2} + \frac{(2.5 - 0)\,(2.5 - 2)}{(1 - 0)\,(1 - 2)}\,k_{j-1}$$

$$+ \frac{(2.5 - 0)\,(2.5 - 1)}{(2 - 0)\,(2 - 1)}\,k_j$$

$$= 0.375\,k_{j-2} - 1.25\,k_{j-1} + 1.875\,k_j \qquad (67)$$

The above extrapolation is repeated for each element of the tangent stiffness to form the complete extrapolated stiffness matrix. This matrix is then factorised and used throughout the increment until convergence to the final solution. Since the extrapolation procedure described above required the tangent stiffness for the previous two increments, this technique can only be applied after the second arc length increment. For the initial two increments either the M.N.R. or the N.R. procedure will have to be used to iterate to convergence.

The usefulness of this extrapolated stiffness strategy rests on the assumptions that

(i) for each element of the tangent stiffness, its value along the solution path does indeed have a relationship than can be modelled closely enough by a 3 point Lagrange interpolation polynomial.

(ii) the extension from the single d.o.f. case to the multi d.o.f. system that by using the gradient (tangent stiffness) at half an arc length increment ahead gives a much closer estimate to the final solution; and

(iii) this better initial estimate will iterated more efficiently to the final solution than the current Newton-Raphson methods.

These assumptions have been validated in Reference [29] for two dimensional frames. The increased efficiency of these extrapolated stiffness strategy over the mNR method is demonstrated in the following numerical example for three dimensional space frames.

7. NUMERICAL EXAMPLES

7.1 CANTILEVER BEAM

Figure 9 depicts a cantilever beam loaded at its free end with a concentrated load. The direction of the load is kept constant in a vertical direction throughout the deformation. A single frame element is used to model the beam. An analytic solution to this problem, obtained through the use of elliptic integrals, is given by Frisch-Fary [46]. It is observed that the results of the numerical analysis using the two dimensional frame program is indistinguishable from the analytical solution.

7.2 WILLIAMS' TOGGLE FRAME

This problem illustrated in Figure 10, has been solved analytically as well as experimentally tested by Williams [6]. In his analytical treatment of the frame, Williams took into consideration the finite change of geometry as well as the effects of the axial forces on the flexural stiffness and the flexural shortening of the members.

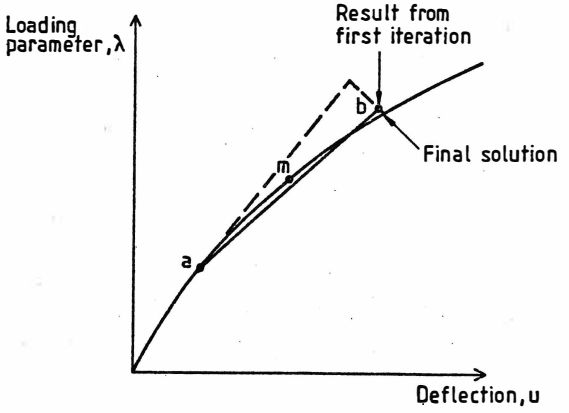

Figure 8. Constant arc length procedure combined with extrapolated stiffness strategy

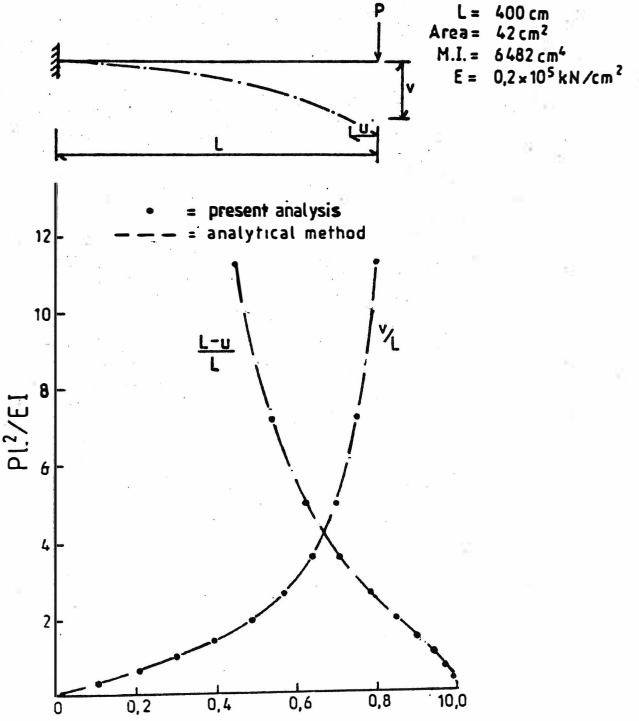

Figure 9. Load deflection curve for cantilever beam

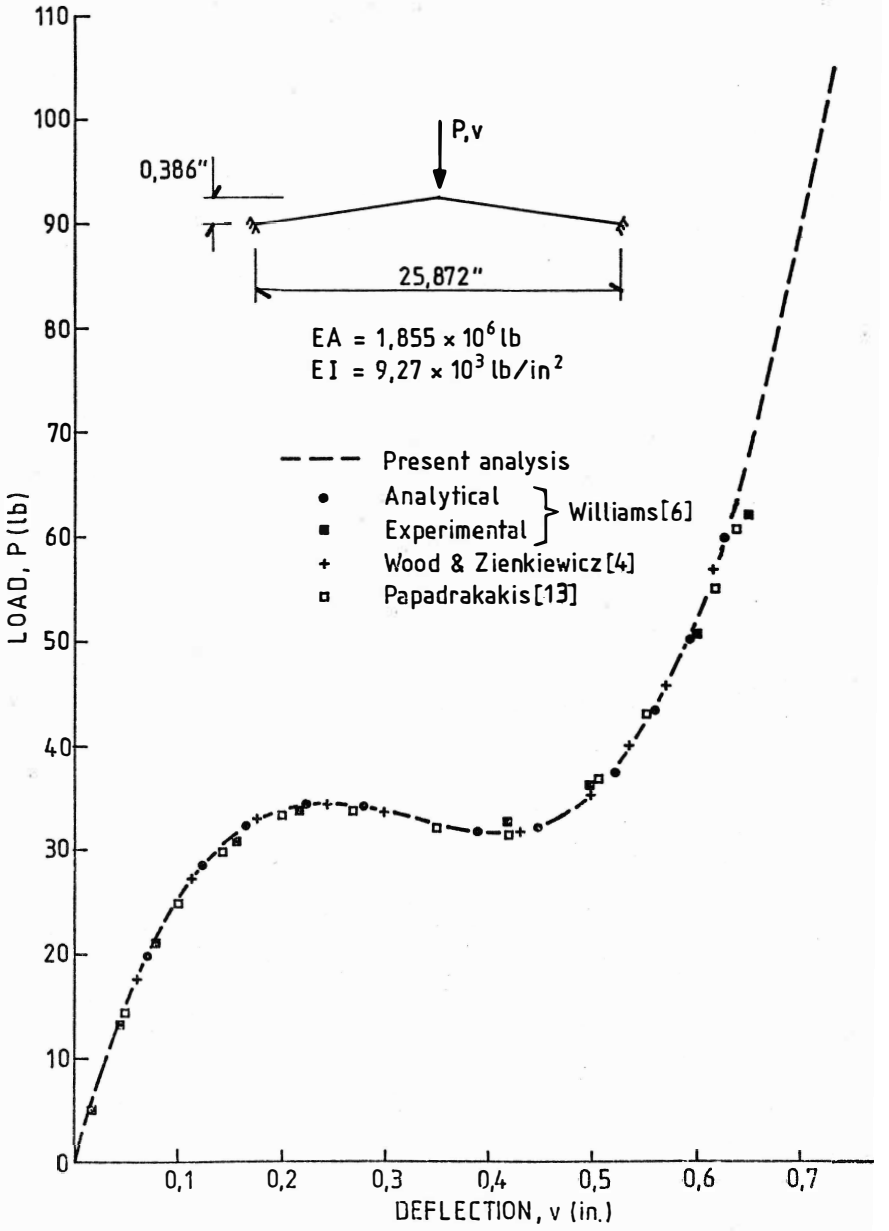

Figure 10. Load deflection curves for Williams toggle frame

Wood and Zienkiewicz [4] have also investigated this problem employing an assumed desplacement finite element approach with five elements per member. Papadrakakis [13] used a 'beam-column' approach to derive the nonlinear equilibrium equations, which were solved through a vector iteration approach.

The authors results, utilising one plane frame element per member, are in very close agreement with the analytical solution of Williams and the finite element solution of Wood and Zienkiewicz.

7.3 TWELVE MEMBER HEXAGONAL SPACE FRAME

This hexagonal frame has been experimentally studied by Griggs [47]. The prebuckling behaviour has also been solved by Chu and Rempetsreiter [10] while Papadrakakis [13] traced the solution into the post buckling range. From Figure 11, it is observed that the present analysis is in agreement with that of Chu and Rempetsreiter in the pre-buckling range. Papadrakakis' curve appears to be in exact agreement with that of the experimental result, which yielded a snap through load 4% lower than that of the writers.

The post-buckling region of the writers' solution path does not correspond exactly with that presented by Papadrakakis. In his formulation, he treated the rotations as a vector and it appears to the writers, therefore, that the validity of his results in the presence of genuinely large rotations, which do occur in the post-buckling range, is doubtful.

Iteration to convergence was achieved using the mNR method and the proposed extrapolated stiffness method. The average number of iterations per arc length was 3.5 for the mNR method and 2.3 for the

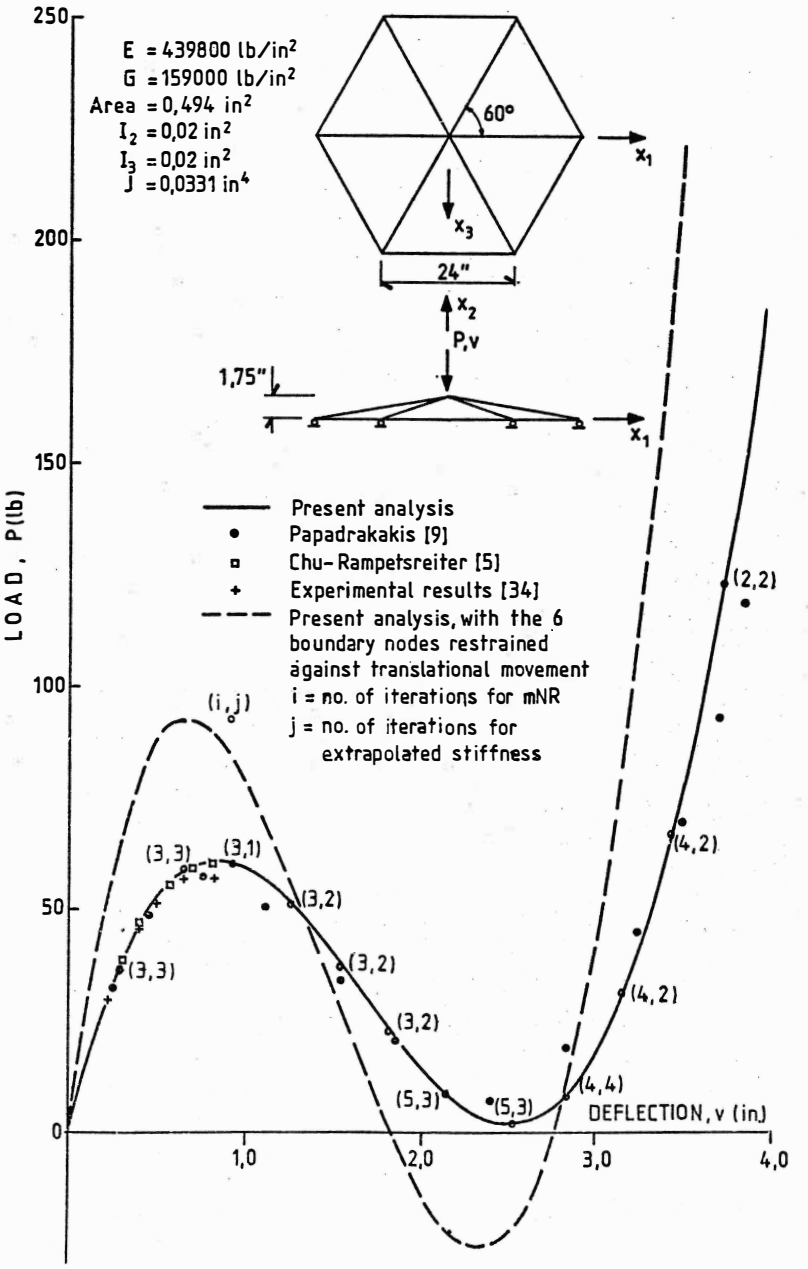

Figure 11. Load-deflection curve for hexagonal frame

extrapolated stiffness strategy. This increased efficiency is further illustrated by the cpu times required for the two runs (implemented on the VAX-11/780 computer), 22.5 secs for the mNR and 17.8 secs for the extrapolated stiffness method.

Next, the structure with the six boundary nodes now restrained against translational movement in all directions, was reanalysed. As shown in Figure 11, this has the effect of yielding a larger snap-through load. In addition, it was observed at the snap-through load that two diagonal elements of the triangularised stiffness matrix changed sign (from positive to negative) at essentially the same load level. This resulted in a positive determinant and would indicate that the matrix is still positive definite if the determinant is used as the criterion for determining it. The incremental stiffness matrix is, however, negative definite at this stage, as is indicated by considering the sign of the incremental work done.

At the lowest point of the post-buckling region, the solution strategy broke down as no real roots could be found for the quadratic of Equation (56). On examination, it was found that at that load level, one of the rotational degree of freedoms exhibited a singularity before it occurred for the vertical displacement of the loaded node. This resulted in a norm measure of the displacement increment due to the residual forces becoming very much larger than that due to the external applied load which yielded the condition of Equation (58). To prevent the applied solution strategy from breaking down, wherever the condition of Equation (58) occurs, iteration is suppressed and only pure incrementation is applied.

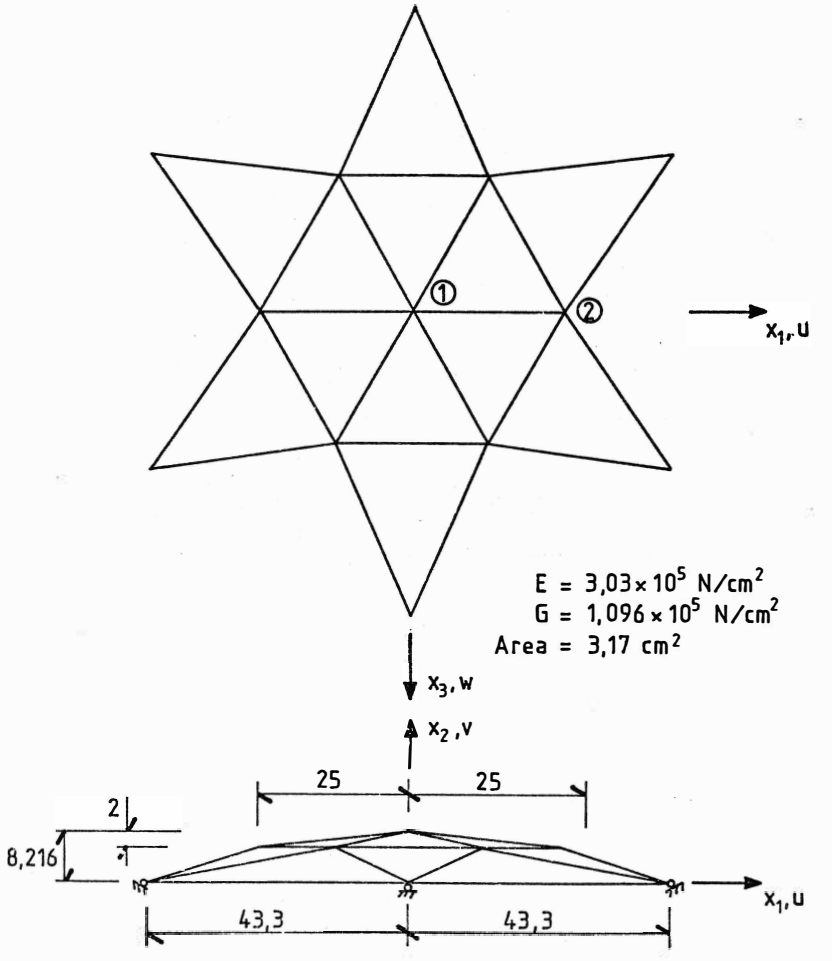

Figure 12(a). Geometry of 24 member star-shaped shallow dome

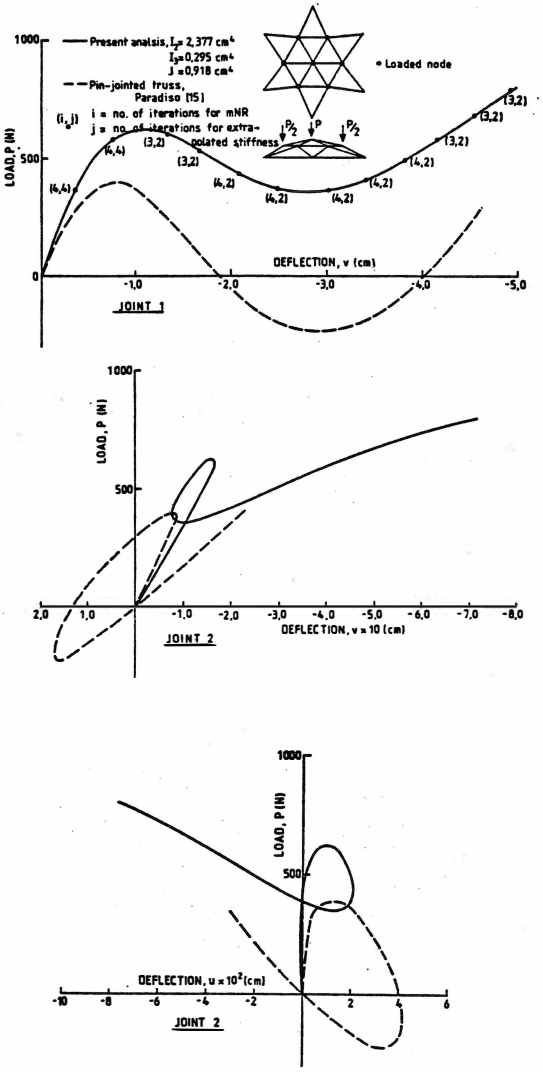

Figure 12(b). Load-deflection curves

7.4 TWENTY-FOUR MEMBER STAR-SHAPED DOME

The structure depicted in Figure 12(a) has been analysed by various authors [13,48,49] as a space truss to trace its load-deflection behaviour into the post-buckling range. Here, the structure is analysed as a space frame and its post-buckling path for the loading condition of Figure 12(b) presented. The supports of the dome are assumed to be pinned and restrained against translational motion.

The average number of iterations per arc length increment is 3.5 using the mNR method and 2.3 utilising the extrapolated stiffness method. The corresponding cpu times used are 46.3 secs for the mNR and 38.0 secs for the extrapolated stiffness technique.

8. CONCLUSION

An updated Lagrangian large rotation formulation of the nonlinear equilibrium equations governing the large deflection of plane and space frames, within the confines of 'beam-column' theory has been presented. A comprehensive survey of the most recent solution strategies available for analysing the post-buckling behaviour of structures was also undertaken. From this review, it was concluded that the arc length strategy due to Crisfield [43] is most robust and efficient, and thus this incremental-iterative method was used in conjunction with the derived system of nonlinear equations to study the post-buckling behaviour of spatial framed structures. The results of the analyses are in good agreement with previously published experimental and analytical work. Modifications to the described strategy to enable it to trace the secondary post-bifurcation path are also discussed.

The solution of the nonlinear equations is expensive in computing time and this is especially so for large scale problems. An extrapolated stiffness method which would reduce the computing time needed to arrive at a particular solution was presented. For the space frames analysed above, it was found to be more efficient than using the conventional mNR method.

For most problems, what is required is the snap-through load without the need to trace the post-buckling path. However, in some cases, for example in studying the effects of a concentrated load on a restricted part of the structure, it is important to obtain information on the nature of the load shedding after the occurrence of a local instability, in order to assess the behaviour of the whole structure. Due to the lack of robust and efficient techniques for critical points, not much attention has been focused on the problem of analysing the post-buckling behaviour of spatial frames. It is hoped that this report will go some way in helping to remedy this situation.

APPENDIX A - NOMENCLATURE

Symbol	Meaning
A	area of cross-section
$\underset{\sim}{a}^{(k)}$	eigenvector
$[\underset{\sim}{A}]$	displacement transformation matrix
$[\underset{\sim}{B'}]$	member rotation matrix
$[\underset{\sim}{B}]$	transformation matrix relating local member forces to member basic forces
$[\Delta\underset{\sim}{B}]$	change in $[\underset{\sim}{B}]$ resulting from $\{\Delta\underset{\sim}{\bar{u}}\}$
$[\underset{\sim}{D}]$	stiffness modification matrix to account for the effect of member forces (two-dimensional frame)
$\frac{dp}{dr}$	generalised gradient of load-displacement curve
E	modulus of elasticity
e	axial displacement of member
$\{\underset{\sim}{\bar{F}}\}$, $\{\underset{\sim}{f'}\}$	intermediate force vector
$\{\underset{\sim}{\bar{F}'}\}$	rotated member local force vector
$\{\Delta\underset{\sim}{F}\}$, $\{\Delta\underset{\sim}{f}\}$	incremented joint force vector
$\{\Delta\underset{\sim}{\bar{F}}_u\}$	variation of the vector $\{\underset{\sim}{\bar{F}}\}$ resulting from incremental displacement $\{\Delta\underset{\sim}{\bar{u}}\}$
$\{\Delta\underset{\sim}{\bar{F}}\}$, $\{\Delta\underset{\sim}{f'}\}$	incremental joint force vector
GJ	torsional rigidity
I, I_m	moment of inertia
$[\underset{\sim}{K}]$, $[\underset{\sim}{k}]$	member basic incremented stiffness matrix
$[\underset{\sim}{\bar{K}}]$	member incremental stiffness matrix in local co-ordinates
$\underset{\sim}{K}$, $\underset{\sim}{K}_i$	tangent stiffness matrix
$[\underset{\sim}{K}_A]$	augmented stiffness matrix
$[\underset{\sim}{K}_G]$, $[\underset{\sim}{k}_G]$	global incremental stiffness matrix

$\underset{\sim}{K}(\underset{\sim}{q}_C + \underset{\sim}{q}_B)$	incremental stiffness matrix corresponding to displacement vector $\{\underset{\sim}{q}_C + \underset{\sim}{q}_B\}$
k_j	j th element of the tangent stiffness matrix stored in a 'skyline' array
k	stiffness of fictitious spring
ℓ	undeformed length parameter
$\Delta\ell$	generalised arc length parameter
M_m, M_{mn}	bending moment
M_t	torsional moment
$[\underset{\sim}{N}]$	stiffness modification matrix to account for the effect of member force (three dimensional frame)
P	axial force
$\underset{\sim}{P}$, $\{\underset{\sim}{P}\}$	external load vector
$\{\Delta P\}$	incremental external load vector
$\left[\underset{\sim}{p}^{(i)}\right]$	end section orientation matrix for end section i
Δp_i	incremental load multiplier
$\{\underset{\sim}{Q}\}$	reference load vector
q	generalised co-ordinates
$\Delta\underset{\sim}{q}^i$	incremental generalised displacement vector at point i
$[R]$	transformation matrix for local convective co-ordinates to global co-ordinates
$\underset{\sim}{R}$	residual force vector
$\underset{\sim}{R}_c$	characteristic load vector
$\underset{\sim}{R}_{ref}$	reference load vector
$[\underset{\sim}{r}]$	member orientation matrix
$\Delta\underset{\sim}{r}$	incremental displacement vector
$\{\underset{\sim}{S}\}$, $\{\underset{\sim}{s}\}$	member force vector
S_o	transverse force
S_p	current stiffness parameter

$\{\Delta\underset{\sim}{S}\}$, $\{\Delta\underset{\sim}{s}\}$	member incremental force vector
ΔS_o	incremental transverse force
$[\underset{\sim}{T}]$	displacement transformation matrix
$\{\underset{\sim}{u}\}$	joint displacement vector
$\{\underset{\sim}{u}'\}$	intermediate displacement vector
u'	relative displacement of member ends measured parallel to undeformed member axis
$\{\Delta\underset{\sim}{u}\}$	incremental joint displacement vector
$\Delta\underset{\sim}{u}$	incremental displacement vector
$\{\Delta\underset{\sim}{u}'\}$, $\{\Delta\underset{\sim}{\bar{u}}\}$	intermediate incremental displacement vector
$\Delta\underset{\sim}{u}_e$	incremental displacement vector due to arbitrary external load increment
$\Delta\underset{\sim}{u}_r$	incremental displacement vector due to residual forces
$\delta\underset{\sim}{u}^{(i)}$	incremental displacement from first iterative cycle to i th iterative cycle
V	potential energy of system
V_{ij}	coefficient matrix of the quadratic form
v'	relative displacement of member ends measured perpendicular to undeformed member axis
$\{\Delta\underset{\sim}{V}\}$, $\{\Delta\underset{\sim}{v}\}$	member incremental displacement vector
ΔW	incremental work
X_1, X_2, X_3	global coordinate axes
x_1, x_2, x_3	member coordinate axes
α	initial inclination of member to global axes
$[\underset{\sim}{\alpha}]$	joint orientation matrix
$[\Delta\underset{\sim}{\alpha}]$	incremental joint orientation matrix
δ_{ij}	kronecker delta
$\Delta\lambda$	incremental load multiplier
Ω_k	eigenvalue

$[\Delta\underset{\sim}{\Omega}]$	incremental joint rotation matrix
θ	norm of stiffness matrix
θ_m, θ_{mn}	member relative end rotation
θ'_m	joint rotation of node m
θ_t	angle of twist of member
ϕ	potential energy
Λ	load reduction factor

APPENDIX B - REFERENCES

1. MALLETT, R.H. and MARCAL, P.V. (1968) "Finite Element Analysis of Nonlinear Structures", Journal of the Structural Division, ASCE, Vol. 94, pp 2081-2105.

2. BERKE, L. and MALLETT, R.H. (1969) "Automated Large Deflection and Stability Analysis of Three-dimensional Structures", in Mar, J. and Liebowitz, H., (eds.), Structures Technology for Large Radio and Radar Telescope Systems, MIT Press, Cambridge, Mass., pp 381-419.

3. POWELL, G.H. (1969) "Theory of Nonlinear Elastic Structures", Journal of the Structural Division, ASCE, Vol. 94, pp 2687-2701.

4. WOOD, R.D. and ZIENKIEWICZ, O.C. (1977) "Geometrically Nonlinear Finite Element Analysis of Beams, Frames, Arches and Axisymmetric Shells", Computer Structures, Vol. 7, pp 725-735.

5. REMSETH, S.N. (1977) "Nonlinear Stratic and Dynamic Analysis of Framed Structures", Computer and Structures, Vol. 10, pp 879-897.

6. WILLIAMS, F.W. (1964) "An Approach to the Nonlinear Behaviour of the Members of a Rigid Jointed Plane Framework with Finite Deflections", Quartly Journal of Mechanically Applied Mathematics", Vol. 17, pp 451-469.

7. JENNINGS, A. (1968) "Frame Analysis Including Change of Geometry", Journal of the Structural Division, ASCE, Vol. 94, pp 627-644.

8. CONNOR, J.J., LOGCHER, D. and CHEN, S.C. (1968) "Nonlinear Analysis of Elastic Framed Structures", Journal of the Structural Division, ASCE, Vol. 94, pp 1525-1547.

9. TEZCAN, S.S. and MAHAPATRA, B.C. (1969) "Tangent Stiffness Matrix for Space Frame Members", Journal of the Structural Division, ASCE, Vol. 95, pp 1257-1270.

10. CHU, K.H. and RAMPETSREITER, R.H. (1972) "Large Deflection Buckling of Space Frames", Journal of the Structural Division, ASCE, Vol. 98, pp 2701-2722.

11. ORAN, C. (1973) "Tangent Stiffness in Plane Frames", Journal of the Structural Division, ASCE, Vol. 99, pp 973-985.

12. ORAN, C. (1973) "Tangent Stiffness in Space Frames", Journal of the Structural Division, ASCE, Vol. 99, pp 987-1001.

13. PAPADRAKAKIS, M. (1981) "Post-buckling Analysis of Spatial Structures by Vector Iteration Methods", Computer and Structures, Vol. 14, pp 393-402.

14. JACOBY, S.L.S., KOWALIK, J.S. and PIZZO, J.T. (1972) Iterative Methods for Nonlinear Optimisation Problems, Prentice-Hall Inc. Englewood Cliffs, New Jersey.

15. POWELL, M.J.D. (1964) "An Efficient Method for Finding the Minimum of a Function of Several Variables Without Calculating Derivatives", Computer Journal, Vol. 7, pp 155-162.

16. FLETCHER, R. and REEVES, C.M. (1964) "Function Minimisation by Conjugate Gradients", Computer Journal, Vol. 7, pp 149-154.

17. BROYDEN, C.G. (1970) "The Convergence of a Doubly-rank Minimisation 2: The New Algorithm", Journal of the Institute of Matematics and its Application, Vol. 6, pp 222-231.

18. FLETCHER, R. (1970) "A New Approach to Variable Metric Algorithms", Computer Journal, Vol. 13, pp 317-322.

19. FLETCHER, R. and POWELL, M.J.D. (1970) "A Rapidly Convergent Method for Minimisation", Computer Journal, Vol. 6, pp 163-168.

20. CRISFIELD, M.A. (1979) "A Faster Modified Newton-Raphson Iteration", Computer Methods and Applied Mechanics and Engineering, Vol. 20, pp 267-278.

21. BRODLIE, K.W. (1977) "Unconstrained Minimisation", in: Jacobs, D., (ed.), The State of the Art in Numerical Analysis, Academic Press, pp 229-268.

22. KAMAT, M.P. and HAYDUK, R.J. (1980) "Energy Minimisation Versus Pseudo Force Technique for Nonlinear Structural Analysis", Computer and Structures, Vol. 11, pp 403-409.

23. CONNOR, J.J. (1969) "Analysis of Geometrically Nonlinear Framed Structures", in Mar, J. and Liebowitz, H., (eds.), Structures Technology for Large Radio and Radar Telescope Systems, MIT Press, Cambridge, Mass., pp 421-443.

24. BERGAN, P.G., HORRIGMOE, G., KRAKELAND, B. and SOREIDE, T.H. (1978) "Solution Techniques for Nonlinear Finite Element Problems", International Journal of Numerical Methods in Engineering, Vol. 12, pp 1677-1696.

25. BERGAN, P.G. (1980) "Solution Algorithms for Nonlinear Structural Problems", Computer and Structures, Vol. 12, pp 497-509.

26. RAMM, E. (1981) "Strategies for Tracing the Nonlinear Response Near Limit Points"; in: Wunderlich, W., Stein, E. and Bathe, K.J., (eds.), Nonlinear Finite Element Analysis in Structural Mechanics, Springer-Verlag, Berlin, pp 63-69.

27. CRISFIELD, M.A. (1982) "Numerical Analysis of Structures", in: Rhodes, J. and Walker, A.C., (eds.), Developments in Twin-Walled Structures, Applied Science Publishers, London.

28. KARAMONANLIDIS, D., HONECKER, A. and KNOTHE, K. (1981) "Large Deflection Finite Element Analysis of Pre and Post Critical Response of Thin Elastic Frames", in: Wunderlich, W., Stein, E. and Bathe, K.J., (eds.), Nonlinear Finite Element Analysis in Structural Mechanics, Springer-Verlag, Berlin, pp 217-235.

29. MEEK, J.L. and TAN, H.S. "A Stiffness Extrapolation Strategy for Nonlinear Analysis", to be published in Computer Methods in Applied Mechanics and Engineering.

30. BELYTSCHKO, T. and SCHWER, L. (1977) "Large Displacement, Transient Analysis of Space Frames", International Journal of Numerical Methods in Engineering, Vol. 11, pp 65-84.

31. SHARIFI, P. and POPOV, E.P. (1971) "Nonlinear Buckling Analysis of Sandwich Arches", Journal of Engineering Mechanics, ASCE, Vol. 97, pp 1397-1411.

32. SHARIFI, P. and POPOV, E.P. (1973) "Nonlinear Finite Element Analysis of Sandwich Shells of Revolution", American Institute of Aeronautics and Astronautics Journal, Vol. 11, pp 715-722.

33. BERGAN, P.G. and SOREIDE, T.H. (1978) "Solution of Large Displacement and Instability Problems using the Current Stiffness Parameter", in: Bergan, P.G., Finite Elements in Nonlinear Mechanics, Tapir, Trondheim, pp 647-669.

34. ARGYRIS, J.H. (1965) "Continua and Discontinua", Proceedings of 1st Conference on Matrix Methods in Structural Mechanics, Wright-Patterson AFB, Ohio, pp 11-189.

35. PIAN, T.H.H. and TONG, P. (1971) "Variational Formulation of Finite-Displacements Analysis", in: De Venbeke, B.F., (ed.), High Speed Computing of Elastic Structures, Liege, Belgium, pp 43-63.

36. YAMADA, Y., IWATA, K., KAKIMI, T., and HOSOMURA, T. (1974) Large Deflection and Critical Loads Analysis of Framed Structures", in: Oden, J.T., (ed.), Computational Methods in Nonlinear Mechanics, University of Texas, Texas, pp 819-829.

CURRENT CIVIL ENGINEERING BULLETINS

4 *Brittle Fracture of Steel — Performance of ND1B and SAA A1 structural steels: C. O'Connor (1964)*

5 *Buckling in Steel Structures — 1. The use of a characteristic imperfect shape and its application to the buckling of an isolated column: C. O'Connor (1965)*

6 *Buckling in Steel Structures — 2. The use of a characteristic imperfect shape in the design of determinate plane trusses against buckling in their plane: C. O'Connor (1965)*

7 *Wave Generated Currents — Some observations made in fixed bed hydraulic models: M.R. Gourlay (1965)*

8 *Brittle Fracture of Steel — 2. Theoretical stress distributions in a partially yielded, non-uniform, polycrystalline material: C. O'Connor (1966)*

9 *Analysis by Computer — Programmes for frame and grid structures: J.L. Meek (1967)*

10 *Force Analysis of Fixed Support Rigid Frames: J.L. Meek and R. Owen (1968)*

11 *Analysis by Computer — Axisymetric solution of elasto-plastic problems by finite element methods: J.L. Meek and G. Carey (1969)*

12 *Ground Water Hydrology: J.R. Watkins (1969)*

13 *Land use prediction in transportation planning: S. Golding and K.B. Davidson (1969)*

14 *Finite Element Methods — Two dimensional seepage with a free surface: L.T. Isaacs (1971)*

15 *Transportation Gravity Models: A.T.C. Philbrick (1971)*

16 *Wave Climate at Moffat Beach: M.R. Gourlay (1973)*

17. *Quantitative Evaluation of Traffic Assignment Methods: C. Lucas and K.B. Davidson (1974)*

18 *Planning and Evaluation of a High Speed Brisbane-Gold Coast Rail Link: K.B. Davidson, et al. (1974)*

19 *Brisbane Airport Development Floodway Studies: C.J. Apelt (1977)*

20 *Numbers of Engineering Graduates in Queensland: C. O'Connor (1977)*

44. WASZCZYSZYN, Z. (1983) "Numerical Problems of Nonlinear Stability Analysis of Elastic Structures", Computer and Structures, Vol. 17, pp 13-24.

45. ISAACSON, E. and KELLER, H.B. (1966) Analysis of Numerical Methods, John Wiley, New York, pp 187-189.

46. FRISCH-FAY, R. (1962) Flexible Bars, Butterworths, London, pp 35-40.

47. GRIGGS, H.P. (1966) "Experimental Study of Instability in Elements of Shallow Space Frames", Research Report, Department of Civil Engineering, MIT, Cambridge, Mass.

48. PARADISO, M. and TEMPESTA, G. (1980) "Member Buckling Effects in Nonlinear Analysis of Space Frames", in: Taylor, C., Hinton, E. and Owen, D.R.J., (eds.), Numerical Methods for Nonlinear Problems, Pineridge Press, Swansea, Wales, pp 395-405.

49. WATSON, L.G. and HOLZER, S.M. (1983) "Quadratic Convergence of Crisfield's Method", Computer and Structures, Vol. 17, pp 69-72.

CIVIL ENGINEERING RESEARCH REPORTS

CE No.	Title	Author(s)	Date
1	Flood Frequency Analysis: Logistic Method for Incorporating Probable Maximum Flood	BRADY, D.K.	February 1979
2	Adjustment of Phreatic Line in Seepage Analysis by Finite Element Method	ISAACS, L.T.	March, 1979
3	Creep Buckling of Reinforced Concrete Columns	BEHAN, J.E. & O'CONNOR, C.	April, 1979
4	Buckling Properties of Monosymmetric I-Beams	KITIPORNCHAI, S. & TRAHAIR, N.S.	May, 1979
5	Elasto-Plastic Analysis of Cable Net Structures	MEEK, J.L. & BROWN, P.L.D.	November 1979
6	A Critical State Soil Model for Cyclic Loading	CARTER, J.P., BOOKER, J.R. & WROTH, C.P.	December 1979
7	Resistance to Flow in Irregular Channels	KAZEMIPOUR, A.K. & APELT, C.J.	February 1980
8	An Appraisal of the Ontario Equivalent Base Length	O'CONNOR, C.	February 1980
9	Shape Effects on Resistance to Flow in Smooth Rectangular Channels	KAZEMIPOUR, A.K. & APELT, C.J.	April, 1980
10	The Analysis of Thermal Stress Involving Non-Linear Material Behaviour	BEER, G. & MEEK, J.L.	April, 1980
11	Buckling Approximations for Laterally Continuous Elastic I-Beams	DUX, P.F. & KITIPORNCHAI, S.	April, 1980
12	A Second Generation Frontal Solution Program	BEER, G.	May, 1980
13	Combined Stiffness for Beam and Column Braces	O'CONNOR, C.	May, 1980
14	Beaches:- Profiles, Processes and Permeability	GOURLAY, M.R.	June, 1980
15	Buckling of Plates and Shells Using Sub-Space Iteration	MEEK, J.L. & TRANBERG, W.F.C.	July, 1980
16	The Solution of Forced Vibration Problems by the Finite Integral Method	SWANNELL, P.	August, 1980
17	Numerical Solution of a Special Seepage Infiltration Problem	ISAACS, L.T.	Septembe 1980
18	Shape Effects on Resistance to Flow in Smooth Semi-circular Channels	KAZEMIPOUR, A.K. & APELT, C.J.	November 1980
19	The Design of Single Angle Struts	WOOLCOCK, S.T. & KITIPORNCHAI, S.	December 1980

CIVIL ENGINEERING RESEARCH REPORTS

CE No.	Title	Author(s)	Date
20	Consolidation of Axi-symmetric Bodies Subjected to Non Axi-symmetric Loading	CARTER, J.P. & BOOKER, J.R.	January, 1981
21	Truck Suspension Models	KUNJAMBOO, K.K. & O'CONNOR, C.	February, 1981
22	Elastic Consolidation Around a Deep Circular Tunnel	CARTER, J.P. & BOOKER, J.R.	March, 1981
23	An Experimental Study of Blockage Effects on Some Bluff Profiles	WEST, G.S.	April, 1981
24	Inelastic Beam Buckling Experiments	DUX, P.F. & KITIPORNCHAI, S.	May, 1981
25	Critical Assessment of the International Estimates for Relaxation Losses in Prestressing Strands	KORETSKY, A.V. & PRITCHARD, R.W.	June, 1981
26	Some Predications of the Non-homogenous Behaviour of Clay in the Triaxial Test	CARTER, J.P.	July, 1981
27	The Finite Integral Method in Dynamic Analysis : A Reappraisal	SWANNELL, P.	August, 1981
28	Effects of Laminar Boundary Layer on a Model Broad-Crested Weir	ISAACS, L.T.	September, 1981
29	Blockage and Aspect Ratio Effects on Flow Past a Circular Cylinder for $10^4 < R < 10^5$	WEST, G.S. & APELT, C.J.	October, 1981
30	Time Dependent Deformation in Prestressed Concrete Girder: Measurement and Prediction	SOKAL, Y.J. & TYRER, P.	November, 1981
31	Non-uniform Alongshore Currents and Sediment Transport - a One Dimensional Approach	GOURLAY, M.R.	January, 1982
32	A Theoretical Study of Pore Water Pressures Developed in Hydraulic Fill in Mine Stopes	ISAACS, L.T. & CARTER, J.P.	February, 1982
33	Residential Location Choice Modelling: Gaussian Distributed Stochastic Utility Functions	GRIGG, T.J.	July, 1982
34	The Dynamic Characteristics of Some Low Pressure Transducers	WEST, G.S.	August, 1982
35	Spatial Choice Modelling with Mutually Dependent Alternatives: Logit Distributed Stochastic Utility Functions	GRIGG, T.J.	September, 1982
36	Buckling Approximations for Inelastic Beams	DUX, P.F. & KITIPORNCHAI, S.	October, 1982

CIVIL ENGINEERING RESEARCH REPORTS

CE No.	Title	Author(s)	Date
37	Parameters of the Retail Trade Model: A Utility Based Interpretation	GRIGG, T.J.	October, 1982
38	Seepage Flow across a Discontinuity in Hydraulic Conductivity	ISAACS, L.T.	December, 1982
39	Probabilistic Versions of the Short-Run Herbert-Stevens Model	GRIGG, T.J.	December, 1982
40	Quantification of Sewage Odours	KOE, C.C.L. & BRADY, D.K.	January, 1983
41	The Behaviour of Cylindrical Guyed Stacks Subjected to Pseudo-Static Wind Loads	SWANNELL, P.	March, 1983
42	Buckling and Bracing of Cantilevers	KITIPORNCHAI, S. DUX, P.F. & RICHTER, N.J.	April, 1983
43	Experimentally Determined Distribution of Stress Around a Horizontally Loaded Model Pile in Dense Sand	WILLIAMS, D.J. & PARRY, R.H.G.	August, 1983
44	Groundwater Model for an Island Aquifer: Bribie Island Groundwater Study	ISAACS, L.T. & WALKER, F.D.	September, 1983
45	Dynamic Salt-Fresh Interface in an Unconfined Aquifer: Bribie Island Groundwater Study	ISAACS, L.T.	September, 1983
46	An Overview of the Effects of Creep in Concrete Structures	SOKAL, Y.J.	October, 1983
47	Quasi-Steady Models for Dynamic Salt-Fresh Interface Analysis	ISAACS, L.T.	November, 1983
48	Laboratory and Field Strength of Mine Waste Rock	WILLIAMS, D.J. & WALKER, L.K.	November, 1983
49	Large Deflection and Post-Buckling Analysis of Two and Three Dimensional Elastic Spatial Frames	MEEK, J.L. & TAN, H.S.	December, 1983

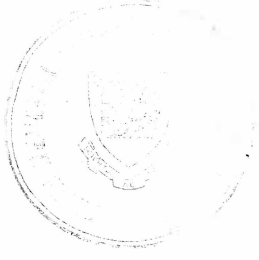

CURRENT CIVIL ENGINEERING BULLETINS

4 *Brittle Fracture of Steel — Performance of ND1B and SAA A1 structural steels: C. O'Connor (1964)*

5 *Buckling in Steel Structures — 1. The use of a characteristic imperfect shape and its application to the buckling of an isolated column: C. O'Connor (1965)*

6 *Buckling in Steel Structures — 2. The use of a characteristic imperfect shape in the design of determinate plane trusses against buckling in their plane: C. O'Connor (1965)*

7 *Wave Generated Currents — Some observations made in fixed bed hydraulic models: M.R. Gourlay (1965)*

8 *Brittle Fracture of Steel — 2. Theoretical stress distributions in a partially yielded, non-uniform, polycrystalline material: C. O'Connor (1966)*

9 *Analysis by Computer — Programmes for frame and grid structures: J.L. Meek (1967)*

10 *Force Analysis of Fixed Support Rigid Frames: J.L. Meek and R. Owen (1968)*

11 *Analysis by Computer — Axisymetric solution of elasto-plastic problems by finite element methods: J.L. Meek and G. Carey (1969)*

12 *Ground Water Hydrology: J.R. Watkins (1969)*

13 *Land use prediction in transportation planning: S. Golding and K.B. Davidson (1969)*

14 *Finite Element Methods — Two dimensional seepage with a free surface: L.T. Isaacs (1971)*

15 *Transportation Gravity Models: A.T.C. Philbrick (1971)*

16 *Wave Climate at Moffat Beach: M.R. Gourlay (1973)*

17. *Quantitative Evaluation of Traffic Assignment Methods: C. Lucas and K.B. Davidson (1974)*

18 *Planning and Evaluation of a High Speed Brisbane-Gold Coast Rail Link: K.B. Davidson, et al. (1974)*

19 *Brisbane Airport Development Floodway Studies: C.J. Apelt (1977)*

20 *Numbers of Engineering Graduates in Queensland: C. O'Connor (1977)*